# Isothermal titration calorimetry as a method to assess the binding kinetics of Syntaxin4, SNAP23, VAMP2 and Munc18c

Andrew Fuller

BSc

Submitted in fulfillment of the requirement for the degree of Master of Science

Institute of Molecular, Cell and Systems Biology

College of Medical, Veterinary and Life Sciences

University of Glasgow

October 2012

Table of Contents:

Acknowledgements

First I would like to thank Gwyn Gould for all his support and guidance throughout the course of this project and Nia Bryant for all her help during my time at Glasgow. I would like to thank all the past and present members of lab 241 who made this project and my day to day life in the lab a fun and enjoyable experience. I owe many thanks to Sharon Kelly and Margaret Nutley for their help with the ITC experiments. I would like to thank my parents for their constant love and support, and finally thank you to Linsey for everything.

List of abbreviations

SNARE - *N*-ethylmaleimide- sensitive factor attachment protein receptor
GLUT4 – Glucose transporter 4
VAMP2 – Vesicle associated membrane protein 2
SM- Sec/Munc
SNAP - Synaptosome associated protein
GSV- GLUT4 storage vesicle
EM – Electron microscopy
GFP – Green fluorescent protein
IRAP - Insulin-responsive aminopeptidase
NSF - *N*-ethylmalemide-sensitive factor
AAA+ - ATPases associated with diverse cellular activities
ER – Endoplasmic reticulum
TGN –Trans golgi network
ΔH – Enthalpy
ITC- Isothermal titration calorimetry
$K_a$ - Association constant
$K_d$ - Dissociation constant
SPR- Surface plasmon resonance
NMR- Nuclear magnetic resonance
2YT - 2x yeast extract and tryptone
SOC - Super Optimal broth with Catabolite repression
TAE – Tris-acetate EDTA
EtBr – Ethidium Bromide
SAP - shrimp alkaline phosphatase
IPTG - Isopropyl-β-D-thiogalactopyranoside
PBS – Phosphate buffered saline
GST - Glutathione S-Transferase
pI – Isoelectric point
FPLC - Fast protein liquid chromatography
SDS-PAGE – Sodium dodecyl sulphate – poly acrylamide gel electrophoresis
ΔTMD – without transmembrane domain
NTA - nitrilotriacetic acid
$His_6$ – 6 x Histadine

Abstract

The ability of humans to regulate their blood glucose using insulin responsive translocation of the glucose transporter GLUT4 to the plasma membrane is key to survival. In the absence of insulin GLUT4 is stored within intracellular vesicles which upon insulin stimulation translocate to the plasma membrane and then fuse with the plasma membrane. This fusion step is driven by a group of proteins known as SNARE proteins more specifically syntaxin 4 and SNAP23 in the plasma membrane and VAMP2 in the vesicle. Located in the plasma membrane and the intracellular vesicles, SNARE proteins are able to form a highly stable complex through their SNARE domains. The binding of SNARE domains to one another brings the vesicle and plasma membrane within close proximity, as the SNARE proteins form a stable complex the energy released is theorised to be sufficient to drive fusion of the vesicle and plasma membrane. The formation of the SNARE complex is regulated by the isolation of the contributing SNARE proteins and by other proteins which can bind both individual SNARE proteins and the SNARE complex as a whole. Munc18c is a member of one such class of proteins, Sec/Munc (SM) proteins and has been shown to bind to syntaxin 4 and the complete SNARE complex of syntaxin 4, SNAP23 and VAMP2. The exact amount of energy released upon the stable binding of SNARE domains in SNARE proteins and their associated regulatory proteins such as SM proteins is still a debated subject. This project aims to elucidate this information by utilising the highly sensitive technique isothermal titration calorimetry and recombinant protein synthesis and purification of the SNARE proteins syntaxin 4, SNAP23 and VAMP2 and the SM protein Munc18c.

# 1 Introduction

## 1:1 Regulation of blood glucose and the role of GLUT4 in type 2 diabetes

The human body has the ability to carefully and precisely regulate blood glucose levels within a narrow range throughout the daily pattern of feeding and fasting. Two hormones play a key role in the regulation of blood glucose: glucagon and insulin which have opposite effects. Insulin is secreted from the pancreas after a meal when blood glucose levels rise and binds to the insulin receptor expressed in skeletal muscle and adipose cells. The binding of insulin to its receptor triggers a signalling cascade downstream which culminates in the translocation of the glucose transporter GLUT4 from sub cellular compartments known as GLUT4 storage vesicles to the plasma membrane. GLUT4 storage vesicles containing GLUT4 proteins are translocated to the plasma membrane and incorporated with the plasma membrane allowing the cell to uptake glucose from the blood and consequently decreasing the blood glucose levels. Since the postulation of the translocation hypothesis and the subsequent cloning of GLUT4 much work has gone into further understanding the intricate mechanisms of insulin mediated GLUT4 translocation and the uptake of glucose from the blood. Importantly the dysfunction of GLUT4 mediated glucose uptake might represent the earliest sign of emerging insulin resistance type 2 diabetes and metabolic syndrome. Given the year on year increase in patients diagnosed with insulin resistance and type 2 diabetes and the associated cost to the health service of treatment, it is of the utmost importance that the details of insulin regulated GLUT4 mediated glucose uptake be well understood as any information could help towards therapeutic targets in the future.

### GLUT4 vesicles

Identified in the 1980's, GLUT4 is the main insulin-responsive glucose transporter in rat adipocytes (Suzuki and Kono, 1980). GLUT4 is a member of a family of facilitative glucose transporters (GLUTs) which is divided into three classes I, II and III based upon similar structural characteristics. Class I: GLUTs 1-4, are the most studied and best understood of the family. Class II consists of GLUT5; a fructose specific transporter, and GLUTs 7,8 and 9. Class III GLUTs include GLUT8, 10 and 12. Class II and III GLUTs are poorly characterised compared to Class I members. The general structure of GLUT4 is shown in figure 1 with cytoplasmic N and C terminals, 12 membrane spanning domains, and both an extracellular and an intracellular loop.

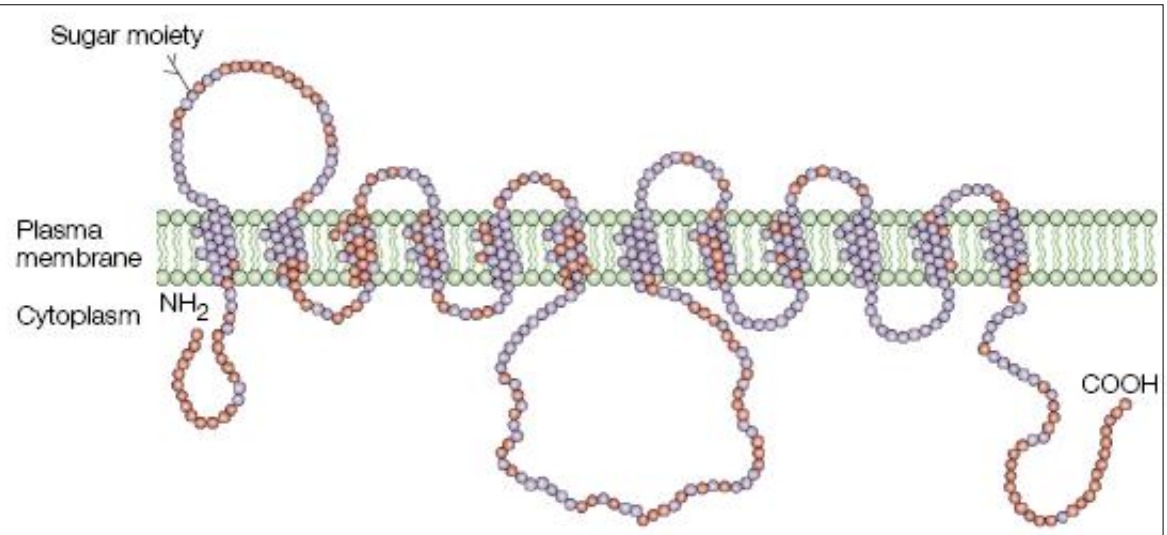


***Figure 1*** *Cartoon representation of GLUT4 structure in the plasma membrane showing cytoplasmic and extracellular loops and 12 membrane spanning domains.* (Bryant, et al., 2002)

Unlike other members of the GLUT family which reside predominantly at the plasma membrane, GLUT4 is sequestered in specialised internal compartments termed GLUT4 storage vesicles (GSVs) under basal conditions excluding it from the plasma membrane (Rea, and James, 1997). The presence of GSVs is difficult to support biochemically or structurally by direct characterisation. It is difficult to distinguish between general endosome recycling compartments and the specialised GSVs as GLUT4 is distributed throughout endosomal compartments and the *trans*-Golgi network (TGN) in basal conditions. *In situ* electron microscopy (EM) studies (Smith, et al., 1991; Ploug, et al., 1998) confirmed earlier work into the distribution of GLUT4 throughout fat and muscle cells and isolated GLUT4 rich membranes, showing that no more than 50% of the intracellular GLUT4 could be recruited to the cell surface in insulin stimulated cells (James D. E., et al., 1988; Zorzano, et al., 1989). Figure 2 shows the distribution of GLUT4 in adipocytes under basal and insulin-stimulated conditions. The presence of GSVs is the commonly held model explaining the insulin responsive compartment of GLUT4 (Pilch, 2007). Figure 3 demonstrates the translocation of GLUT4 from the cytoplasm to the cell membrane upon insulin stimulation using GFP tagged GLUT4 in differentiated 3T3L1 adipocytes. This clearly demonstrates the movement of GLUT4 upon insulin stimulation as very little green GFP signal can be observed within the cytosol of the insulin stimulated cell when compared to the cytosol of the cell under basal conditions

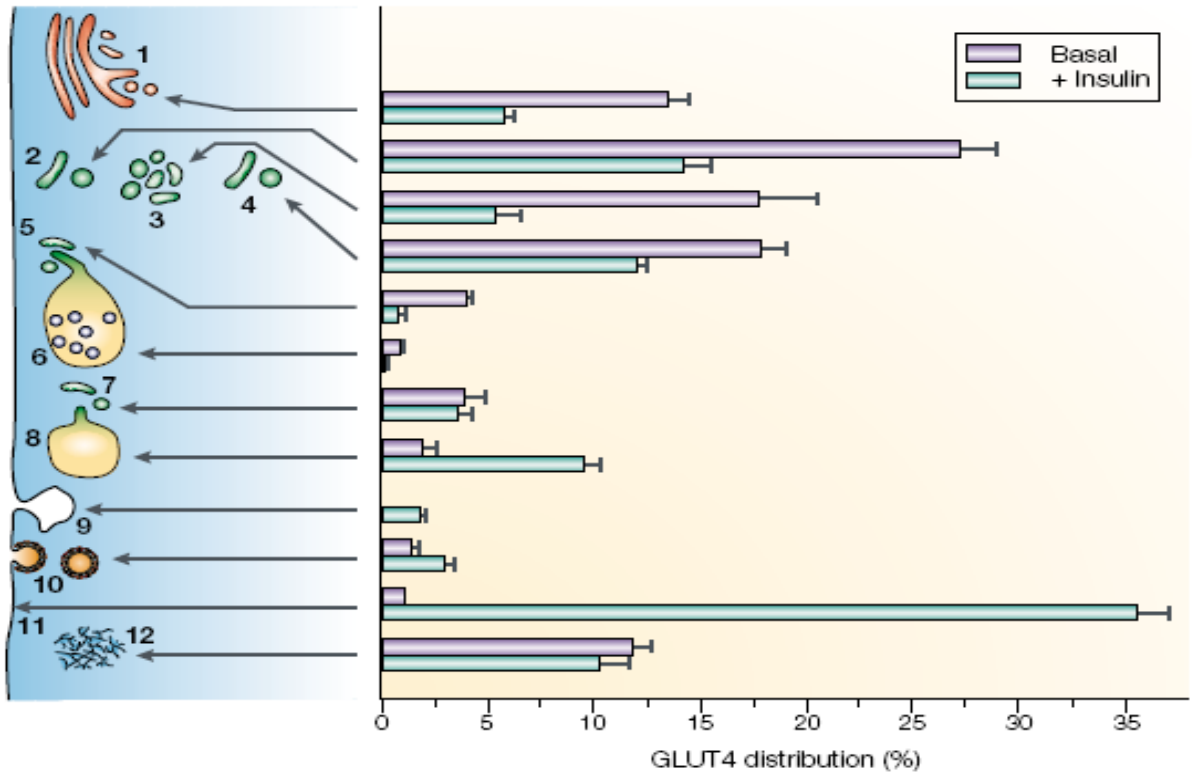


***Figure 2**, Relative GLUT4 distribution throughout organelles of cells from non-stimulated and insulin-stimulated brown adipose tissue.1) trans-*Golgi network *(TGN) 2) tubule-vesicular (T-V) elements located underneath the plasma membrane 3) clusters of T-V elements, 4) T-V endosomal vacuoles(6-7) T-V elements connected or close to early endosomal vacuoles 8-9) noncoated invaginations of the plasma membrane 10) coated pits and vesicles 11) plasma membrane 12) cytoplasm.* (Bryant, et al., 2002)

GLUT4 is not the only constituent of GSVs. The other major constituent is the insulin-responsive aminopeptidase (IRAP), an enzyme which catalyses the cleavage of vasopressin, oxytocin and acts as a receptor for angiotensin IV. Mice with tissue-specific ablation of IRAP show decreased levels of GLUT4 despite maintaining normal glucose homeostatis. Also located within GSVs is the v-SNARE (*N*-ethylmaleimide- sensitive factor attachment protein receptor) VAMP2 (vesicle associated membrane protein) which is thought to mediate GSV fusion with the plasma membrane (Grusovin, and Macaulay, 2003) and sortilin. The distribution of sortilin is similar to IRAP with 50% of the total sortilin protein found in GSVs. It has also been proposed that sortilin is necessary and sufficient for GSV formation (Shi, and Kandror, 2005).

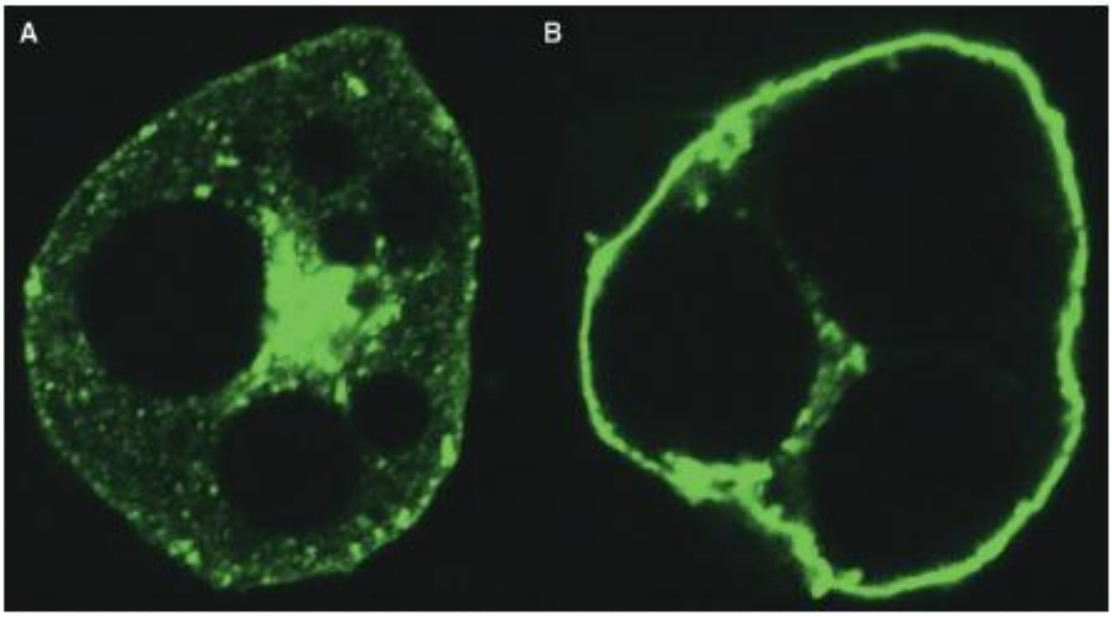


***Figure 3***. *Insulin stimulation results in the translocation of GLUT4 from intracellular storage sites to the plasma membrane. Differentiated 3T3L1 adipocytes were transfected with a GLUT4-enhanced green fluorescent protein fusion construct and then incubated in the absence (A) or presence (B) of insulin for 30 min. The cells were fixed and subjected to confocal fluorescent microscopy* (Watson et al., 2004)

1:2

SNARE proteins

The movement of cargo between membrane bound organelles and the plasma membrane is a feature of all eukaryotic cells. The fusion of vesicles to any membrane requires very high levels of specific control to allow the cell to react to its environment and to respond to internal and external stimuli transporting various specific cargos around the cell to the correct destination. The interaction of proteins that function in the control of vesicle transport and fusion is well reported and is still the focus of much research.

Since their initial characterization in the 1980s in yeast, SNAREs have been identified as key elements in membrane fusion. The popular model for SNARE mediated membrane fusion suggests that SNARE proteins are localised in opposing membranes and drive membrane fusion by using the free energy that is released during the formation of a four helix bundle. The formation of the bundle leads to a tight connection of the membranes and eventual membrane fusion (Jahn and Scheller, 2006). This four helix bundle known as the SNARE complex has been characterised using neuronal SNAREs as shown in figure 4

1:2:1

SNARE protein structure

SNARE proteins belong to a protein superfamily which has conserved SNARE motifs- a stretch of 60-70 amino acids that are arranged in heptad repeats of hydrophobic residues arranged to position all the hydrophobic repeats on the same face of an alpha helix structure (Weimbs et al., 1997). Most SNARE proteins have a C-terminal transmembrane domain connected to SNARE domains by a short linking peptide and independently folded N-terminal domains, although there are members of the SNARE family that lack a transmembrane domain such as the mammalian SNAP-25 (25kDa-synaptosome associated protein), or complex N-terminal domains (Jahn and Scheller, 2006)

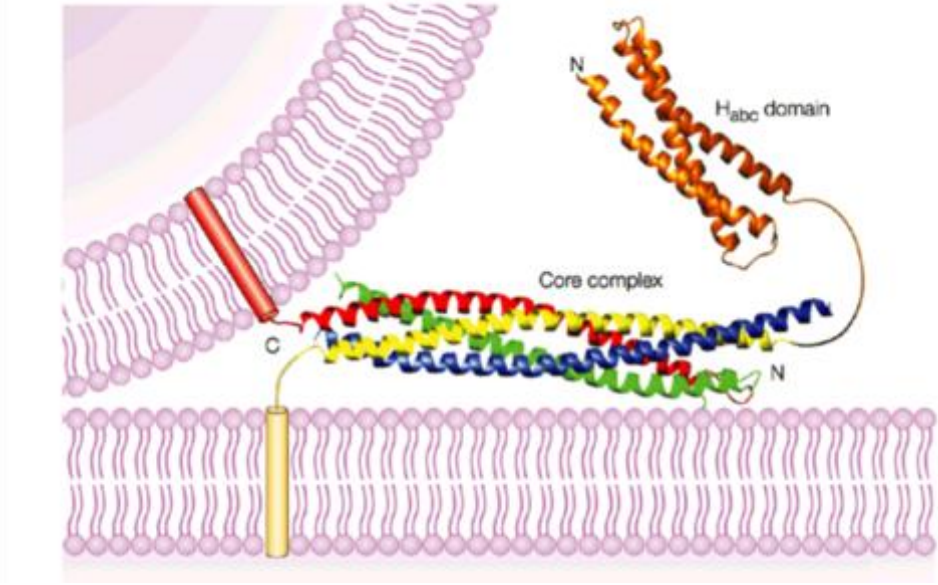


***Figure 4*** *Ribbon diagrams represent the crystal structure of the characteristic 4 helix neuronal SNARE complex with the N terminal $H_{abc}$ domain (orange) of syntaxin1 also shown. Syntaxin1 is shown in yellow is anchored by transmembrane domain (yellow cylinder) in the plasma membrane, SNAP23 shown in blue/green, VAMP1 shown in red is anchored in the vesicular membrane by its transmembrane domain (red cylinder). (Yamaguchi et al 2002).*

The general structure of SNARE proteins, and how SNARE motif structure enables membrane fusion, has been identified through study of the crystal structures of distantly related SNAREs. As mentioned above SNAREs are present on the cytosolic surfaces of vesicles and target membranes. It was previously thought that SNAREs on vesicles and those on target membranes were separated and their function limited to one membrane or the other, leading to the terminology of v-SNAREs (vesicle-SNAREs) and t-SNARES (target-SNAREs). A more precise nomenclature has arisen however as classification according to vesicle or target is not clear (some SNAREs function on both the vesicle and target membrane of one trafficking system). Single SNARE motifs are reasonably unstructured, however when cognate ‘donor’ and ‘acceptor’ SNARE motifs come into contact an incredibly stable heterotetrameric helical core forms. Each of the four alpha helices in the bundle is

contributed by a different SNARE motif however not necessarily a different SNARE protein as some SNARE proteins such as SNAP-25 have multiple SNARE domains(Wang et al., 2008). The crystal structure of the neuronal syntaxin1a SNARE complex showed four helices in this conformation but also showed a surprising central polar layer termed the 'zero' layer comprising of 4 hydrophilic amino acid residues in an otherwise hydrophobic core (Sutton et al., 1998). This hydrophilic layer is formed by three glutamine residues (Q) and one arginine residue (R).

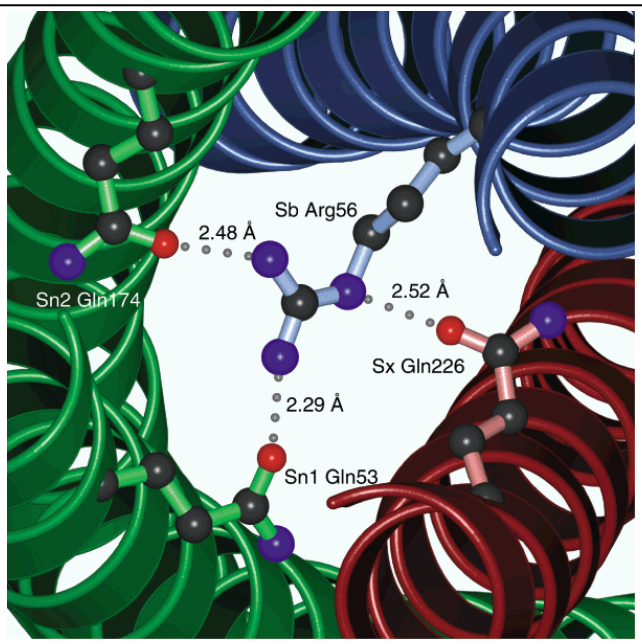


***Figure 5**, The ionic '0' layer of the synaptic fusion complex Side chains involved in the layer are shown as balls and sticks; backbone is shown as a ribbon. The total buried surface area for the sidechain atoms in this layer is 742 Å (Sutton et al., 1998)*

The formation of this ionic layer allowed each SNARE to be labelled more accurately as either a Q-SNARE or an R-SNARE depending on the contribution of a glutamine helix or the arginine respectively. The function of the ionic '0' layer, shown in figure 5, is an ongoing area of research and is thought to have several likely roles: the ionic layer could prevent incorrect alignment of the four helices, the formation of the ionic layer prevents more than one R-SNARE contributing to the complex; however SNARE complexes can be formed exclusively of Q-SNARE motifs and these can function *in vivo* (Katz and Brennwald, 2000). Q-SNARE proteins can be further defined as either $Q_a$ $Q_b$ or $Q_c$ to further classify the donation of each SNARE motif to the four helix bundle. $Q_a$ SNAREs or syntaxins are often membrane bound by a C-terminal transmembrane domain and often contain autonomously folded N-terminal domains which are discussed in the next section. $Q_b$ and $Q_c$ SNARE domains can be donated either by individual proteins meaning 4 separate SNARE proteins form the complex,

by the same SNARE protein as in the previously mentioned SNARE complex of syntaxin1a, SNAP-25 and VAMP1 being R-SNAREs.

1:2:2

SNARE protein N-terminal domains:

The autonomously folded domains at the N-terminus of SNARE proteins are varied. $Q_a$/syntaxins possess a three helical bundle made up of $H_a$, $H_b$ and $H_c$ preceded by an N-terminal domain shown in diagrammatic form in figure 7. $H_{abc}$ domains can function to inhibit SNARE complex assembly by forming a closed formation such as that observed in the neuronal syntaxin, syntaxin1a (Dietrich et al., 2003). This is not always the case as some SNARE proteins that have $H_{abc}$ domains do not show any interaction of these with their C-terminus. It is believed however that SNARE proteins must be in an open conformation to allow SNARE complex formation. Specific protein regulators can bind and open SNARE proteins such as members of the Sec1/Munc-18-related family (SM). SM proteins have been shown to stabilise the closed conformation of SNARE proteins such as the protein Sly1p which binds with the N-terminus of syntaxin 5 and 18 (Yamaguchi et al., 2002). Other N-terminal regions are described in figure 6 below

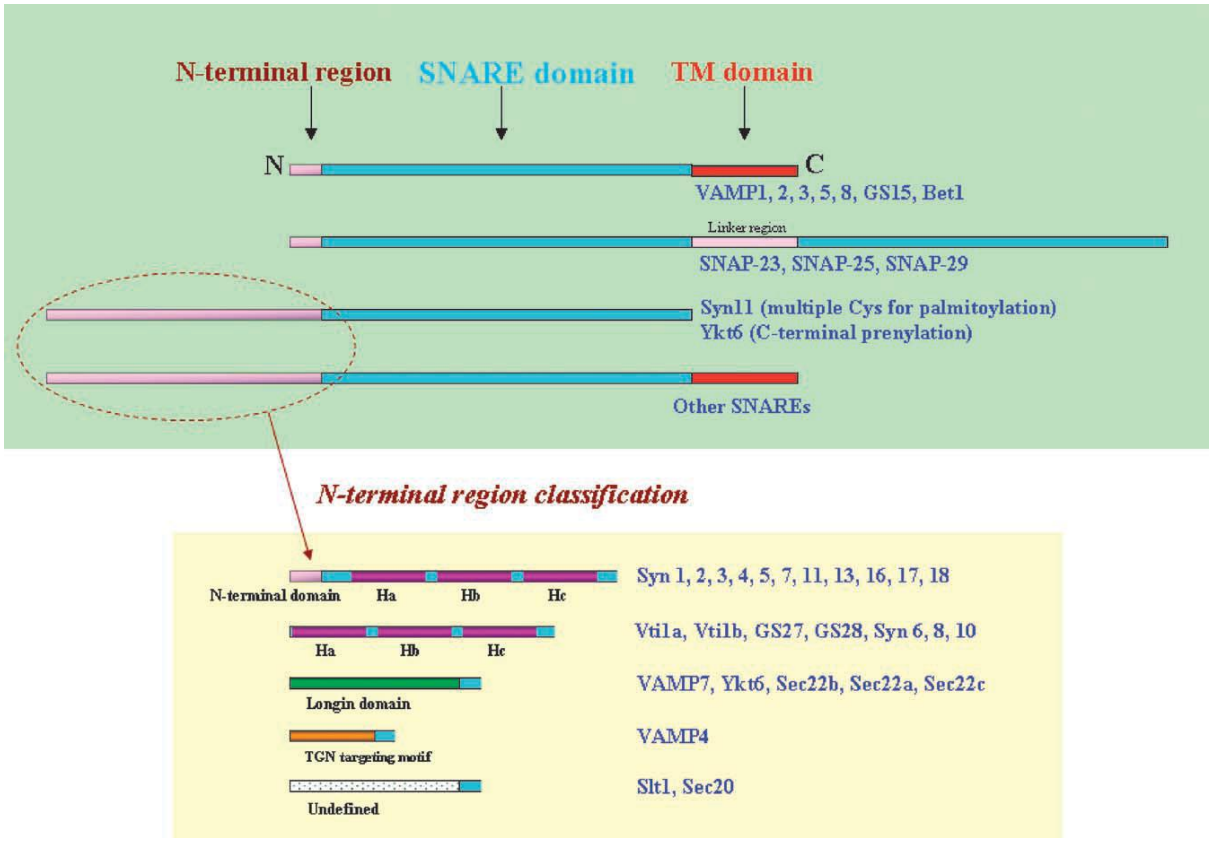


***Figure 6*** *The general structural frameworks of different SNAREs. SNARE domain shown in blue N-terminal region shown in pink in top panel, and shown in more detail in bottom panel. SNARE proteins with corresponding structures are labelled accordingly* (Hong, 2005) *Syn (Syntaxin), TM (transmembrane).*

a)

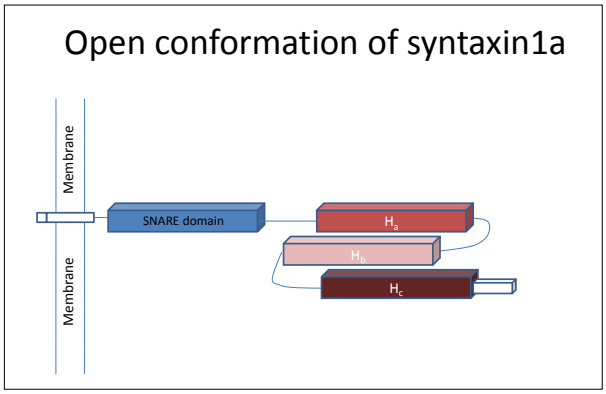


b)

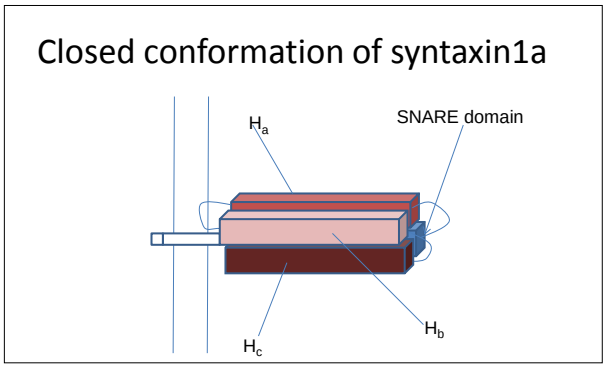


***Figure 7*** *Schematic diagram of syntaxin1a showing the C-terminal transmembrane domain connected to the characteristic SNARE domain. The autonomously folded N-terminal domain shown in open conformation in a) is capable of forming a closed confirmation b) thus preventing SNARE complex assembly.*

1:3

SNARE-mediated membrane fusion.

The action of SNARE proteins in membrane fusion is still not clearly defined. Much work has been carried out *in vitro* and *in vivo* to try to define the specific role SNAREs have in membrane fusion. Many experiments have been carried out looking at the interaction of Q-SNAREs syntaxin1, SNAP-25 and the R-SNARE VAMP-2 which functions in synaptic vesicle

fusion. The crystal structure of this complex was solved (Sutton et al., 1998) leading to much further work assessing all the aspects of SNARE complex formation and the role of SNARE proteins in membrane fusion.

Early work into SNAREs highlighted an interaction with the cellular ATPase NSF (*N*-ethylmalemide-sensitive factor) and it was proposed that it was the interaction of NSF on assembled SNARE complexes that gave the energy to drive membrane fusion (Sollner et al., 1993). It was later determined that NSF was not involved in fusion, rather that the assembly of SNARE motifs into a complex provided sufficient energy for membrane fusion (Mayer et al., 1996). The role of NSF in the pathway is in the disassembly of the stable SNARE complex thus freeing up SNARE proteins for another round of fusion. The widely accepted mode of action of SNAREs during membrane fusion is described in figure 8.

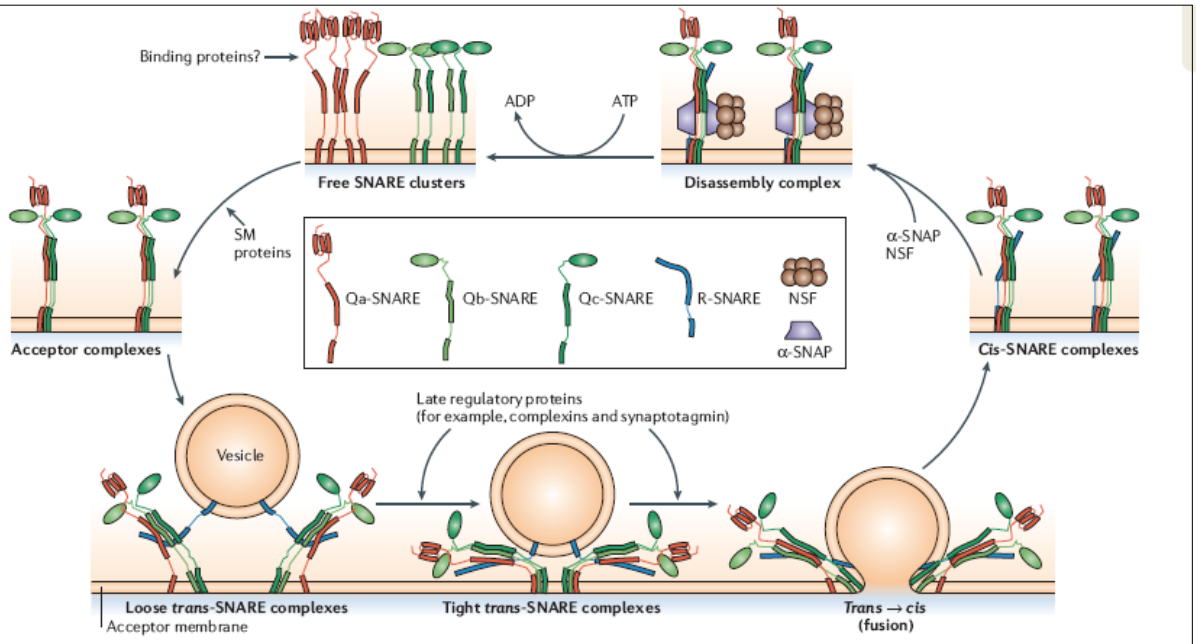


***Figure 8*** *The SNARE conformational cycle during vesicle docking and SNARE complex assembly relies on the formation of a partially helical $Q_{abc}$ intermediate which acts like an acceptor for the R-SNARE. The $Q_a$, $Q_b$ and $Q_c$ SNAREs contact seems to start by contact with the N-terminal region of the SNARE motifs and proceeds to associate in a zipper-like fashion towards the C-terminus fusion* (Jahn and Scheller, 2006)

The work done by (Fasshauer and Margittai, 2004) confirms this theory as truncations in the N-terminal, and not the C-terminal, region of the SNARE motif prevented complex formation. These acceptor complexes are very reactive and subsequently difficult to analyse *in vitro*. The formation of the $Q_{abc}$ intermediate is controlled in part by SM proteins which will be discussed in more detail later. Once the R-SNARE is recruited a loose *trans* SNARE complex is assembled where the association is restricted to the N-terminal region of the SNARE motifs. This is then 'zipped up' towards the C-terminus forming a tight *trans* SNARE

complex controlled by proteins such as complexins and synaptotagmin. After this stage the fusion pore is opened and the complex shifts into a *cis*-configuration which are targets for the AAA+ (ATPases associated with various cellular activities) protein NSF.

1:4

Controlling SNARE mediated membrane fusion: the role of SM proteins.

SM proteins were linked to membrane fusion after the isolation of a 67kDa protein bound to syntaxin1 in the neuronal SNARE complex. After amino-acid sequencing and complementary DNA cloning was revealed to be encoded by the mammalian homologue of a *Caenorhabditis elegans* gene *unc-18*. The *C. elegans* gene when mutated leads to a paralytic phenotype and accumulation of acetylcholine implying a link between *unc-18* and neurotransmitter release (Hata et al., 1993) indicating a role for the protein in vesicle fusion. SM proteins are arch-shaped structures with a conserved region of around 600 amino acids (Misura et al., 2000). Their interaction with SNARE complexes and more specifically with syntaxins has been the focus of much research. The neuronal SNARE complex of syntaxin1, SNAP-25 and synaptobrevin/VAMP and the interactions of the cognate SM protein Munc18-1 have been studied and the relationship of the SM protein and syntaxin has been extrapolated to reflect SM-syntaxin/SNARE complex interactions in other mammalian vesicle fusion systems. SM proteins interact with SNARE proteins in multiple ways, SM proteins can bind to the $H_{abc}$ domain and SNARE motif of sytaxin1 which clasps the SNARE protein in its closed conformation making the syntaxin SNARE motif unable to form complexes (fig 7) (Misura et al., 2000). The SM protein interacts with 4 helices in this mode of binding, three from the conserved $H_{abc}$ domain and one from the conserved SNARE motif. This binding was the earliest interaction of SNARE and SM proteins to be discovered and led to suggestions that SM proteins were negative regulators of syntaxins. Later work showed that deletion of the major synaptic SM protein Munc18-1 inhibited exocytosis showing that SM proteins may therefore not only be negatively regulating SNAREs (Brenner, 1974). The role of SM proteins was further confused when work on the yeast plasma membrane syntaxin Sso1p showed it also adopted a closed conformation (Nicholson et al., 1998) while the yeast syntaxin Vam3p, essential for vacuolar fusion, did not, despite having an N-terminal 3 helical domain. Further evidence than the ‘closed syntaxin’ interaction was not the only form of binding was shown as Vam3p also does not require its N-terminal three helix domain to interact with its cognate SM protein Vps33p (Dulubova et al., 2001). Therefore the binding of SM proteins with syntaxins in a closed conformation is not the exclusive mode of binding or a universal feature of SM-syntaxin interaction and probably meets the specific requirements of regulated exocytosis (Deak et al., 2009).

A second mode of binding between SM proteins and SNAREs involves an interaction between the short N-terminal peptide sequence present in SNARE proteins. This interaction is conserved between yeast and mammals throughout the endoplasmic reticulum (ER), Golgi, trans-Golgi network (TGN) and early endosomes (Deak et al., 2009). The N-terminal binding also provides an explanation for the ability of SM proteins to promote fusion as an interaction of N-terminal domains (N-terminal lobe of SM, N-terminal short peptide of syntaxin) allows the arch shaped body of the SM protein to interact with the SNARE 4 helix complex and play a part in membrane fusion.

1:5

Syntaxin 4 and Munc18c function in GLUT4 vesicle fusion

Syntaxin 4 and SNAP23 are the only Q-SNAREs that have been associated with GLUT4 insulin-stimulated translocation in adipocytes (Rea et al., 1998). Syntaxin4 has the same basic structure as syntaxin1 with a conserved SNARE domain and an N-terminal three helix $H_{abc}$ domain which can fold back and bind with the SNARE domain forming a closed conformation. SNAP-23 shares close homology with SNAP-25 containing two SNARE motifs and embedded into the plasma membrane by palmitoylated sites between the SNARE domains. Mammals utilise multiple R-SNAREs/VAMPs in different trafficking pathways. The main focus of study with regards to GLUT4 vesicle fusion has been VAMP2 however VAMP2 is not the only R-SNARE capable of allowing vesicle docking and subsequent insertion of GLUT4 into the cell membrane. Using knockout mice, proteolytic cleavage of VAMP proteins and total internal reflection fluorescence microscopy Zhao et al (Zhao et al. 2009) showed functional redundancy between VAMP2, VAMP3 and VAMP8 all of which were able to drive GLUT4 vesicle docking and fusion. The SNARE complex forms and generates fusion as described above; three SNARE motifs are associated together on the plasma membrane two from SNAP-23 and one from syntaxin4. VAMP2 is located on GLUT4 vesicles and transports to the plasma membrane donating the final SNARE domain to the complex which drives membrane fusion. This process is regulated by SM protein interaction with syntaxin4.

The SM protein involved is Munc18c which preferentially binds to syntaxins 2 and 4 (Tellam et al., 1997) forming a heterodimer with syntaxin4. Munc18c has been shown not to associate with SNAP-23 but has shown to bind to VAMP2 *in* vivo (Brandie et al., 2008) and also associate with the assembled ternary SNARE complex. Munc18c binds to the N-terminal peptide of syntaxin4 similar to the interaction of yeast Sed5p N-terminal peptide with its cognate SM protein Sly1p (Bracher and Weissenhorn, 2002). The crystal structure of this binding has been solved and is shown below in figure 9. The N-terminal peptide of both Sed5p and syntaxin4 is predominately helical and in both cases the cognate SM protein

interacts with a short segment of the roughly 30 residue peptide. The interaction involves the first 8 residues in syntaxin4 and the first 10 in Sed5p. The interactions between Munc18c, Sly1p and their respective syntaxins syntaxin4 and Sed5p involve two residues in this short segment of the N-terminal peptide: an arginine in a DRT motif (Arg-4 of sytaxin4 and Arg-6 of Sed5p), and a hydrophobic residue (Leu-8 of syntaxin4 and Phe-10 of Sed5p), both residues are highly conserved. The N-terminal peptide of the syntaxin fits into a hydrophobic pocket on the SM protein. The formation of this pocket, by 5 conserved amino acids, is vital to allow for successful binding. Mutations of key residues in this pocket prevents binding in both Sly1p-Sed5p and syntaxin4-Munc18c interactions (Dulubova et al., 2002), (Latham et al 2006). The formation of the syntaxin4-Munc18c heterodimer promotes SNARE complex formation suggesting a positive regulation role for Munc18c in GLUT4 vesicle fusion (Hu et al., 2007). Munc18c is also proposed to interact with syntaxin4 binding its $H_{abc}$ domain and SNARE domain clamping syntaxin4 in its closed conformation allowing further negative control of the system. This mode of binding has not been solved for syntaxin4/Munc18c using crystallography but has been shown of the neuronal syntaxin1a and its cognate SM protein Munc18-1 (Misura et al., 2000). Work has been carried out by Aran et al (Aran et al 2009), into both binding modes of Munc18c with syntaxin4 and showed using a liposome fusion assay data supporting the binding of Munc18c to the four helices of syntaxin4 $H_{abc}$ domain and SNARE domain. Two separate modes of binding could explain how Munc18c both negatively and positively regulates SNARE complex formation.

1:6

SNARE protein binding kinetics

The thermodynamics of SNARE protein complex formation and the subsequent binding of SM proteins has been analysed using the neuronal SNARE proteins: syntaxin1a, SNAP25 and VAMP1 as a model. SNARE protein complex formation and vesicle fusion, like all biophysical processes are driven by the molecular interactions of the proteins involved. The detailed understanding of these molecular interactions gives further information on the changes in enthalpy and entropy when proteins bind to one another. A useful method of obtaining information on protein thermodynamics is to use isothermal titration calorimetry (ITC). This technique provides measurements of the changes in temperature inside a thermostatically controlled cell containing one protein of interest upon repeated injections of a second protein. The amount of energy required to maintain a stable temperature inside the cell is recorded and from these data the binding enthalpy $\Delta H$, the equilibrium binding affinity $K_a$ and the dissociation constant $K_d$ as well as the stoichiometry (*n*). Using only the SNARE domains from the neuronal SNARE proteins Wiederhold and Fasshauer (Wiederhold and

Fasshauer 2009) assessed the affinity of each individual SNARE domain for each other. The authors observed a large enthalpy change within the assembly of the SNARE complex of roughly 110kcal/mol, they also saw a high affinity of SNAP25 and syntaxin1a which first forms a stable 1:1 heterodimer with a $K_D$ of around 5nM followed by a second syntaxin1a molecule binding with a much lower affinity of around 234nM. By injecting SNAP25 into a mixture of syntaxin1a and VAMP1 the authors showed the highest enthalpy change and were able to show that the formation of the ternary SNARE complex was a two step process with VAMP1 binding to preassembled syntaxin1a – SNAP25 heterodimers.

The binding kinetics of SNARE protein interactions have also been assessed using other in vitro molecular techniques such as: Surface Plasmon Resonance (SPR), NMR spectroscopy, and single-molecule force spectroscopy. The use of such techniques, along with ITC, has given a large amount of information regarding the specificity of SNARE protein binding. Jewell et al showed using SPR that the $K_D$ of Munc18c for syntaxin4 was 32nm. The authors also showed a fast association rate and a slow dissociation rate, indicative of a low free energy barrier for the formation of Munc18c and syntaxin4 complex with a high free energy barrier for dissociation indicating that the binding of Munc18c and syntaxin4 is exothermic (Jewell et al 2008). This result can be compared to ITC data shown by Deak et al who assessed the binding kinetics of Munc18a with syntaxin1a showing a $K_D$ of 7.5 (+/- 2.7)nm (Deak et al 2009). The higher affinity of Munc18a for syntaxin1a between these two experiments is interesting but care must be taken when directly comparing these two results as both use not only a different technique to generate the result but also different constructs and purification procedures to generate the proteins used. NMR spectroscopy has been utilised also to elucidate the binding of SNARE proteins to each other and to their cognate SM protein. This was also accomplished by Deak et al who used NMR spectroscopy in conjuction with $^{13}C$ and $^{15}N$ labelling to identify simultaneous binding of Munc18a and complexin-1 to the assembled neuronal SNARE complex (Deak et al 2009). This is important in the context of neuronal vesicle fusion as complexins act at the calcium triggering step of neurotransmitter release.

The aim of this project was to attempt to evaluate, using the ITC method, the affinity of the SNARE proteins: syntaxin4, SNAP23, VAMP2 and the SM protein Munc18c which are involved in GLUT4 vesicle fusion. The use of ITC and the solubilised forms of SNARE proteins is a reductionist approach. *In vivo,* other interacting proteins play a role in SNARE complex formation as do the structure of the membrane and the interaction of the transmembrane domains which anchor the SNARE proteins. These other factors cannot be easily accounted for using ITC and therefore ITC alone cannot give the complete answer on

membrane fusion. However the knowledge that can be obtained with regards to the specific interactions between the SNARE and SM proteins involved in GLUT4 vesicle exocytosis is extremely valuable. This knowledge can be combined with what is already been established using vesicle fusion assays to allow much closer understanding of the precise amount of energy that can be released by the binding of SNARE and SM proteins to each other. By using previously generated mutants of SNARE proteins produced and purified from *E. coli* this project also aimed to assess the specific affinity of SM protein Munc18c for the SNARE complex, and Munc18c for syntaxin 4 protein. Using ITC to test the correct combinations of mutants and Wildtype proteins can provide a large amount of novel information on these interactions.

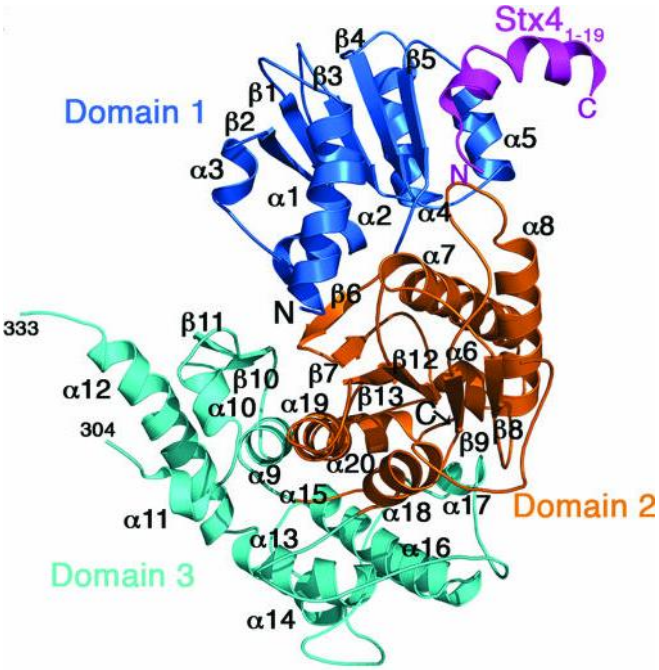


***Figure 9*** *Structure of Munc18c/Syntaxin 4(Stx4$_{1–19}$) proteins. (a) The Munc18c/Stx4$_{1–19}$ complex showing domain 1 (residues 1–138) in dark blue, domain 2 (residues 139–250 and 476–584) in orange, and domain 3 (residues 251–475) in cyan. Stx4 residues 1–19 are shown in magenta. Helices are shown as coils, and strands are shown as arrows. N and C termini and secondary structure elements are labelled.*(Hu et al., 2007)

2:0

Methods

2:1

Bacterial growth media

| | |
|---|---|
| 2YT | 1.6% (w/v) tryptone, 1% (w/v) yeast extract powder, 0.5% (w/v) NaCl |
| Terrific broth | 1.2% (w / v) tryptone, 2.4% (w / v) yeast extract, 0.4% (v / v) glycerol, 0.017 M $KH_2PO_4$, 0.072 M $K_2HPO_4$. Purchased from Melford Labs Ltd |
| SOC | 2% (w / v) tryptone, 0.5% yeast extract, 10 mM NaCl, 2.5 mM KCl, 10 mM $MgCl_2$, 10 mM $MgSO_4$, 20 mM glucose |

If solid media was required 2%(w/v) micro agar was added to bacterial growth media prior to sterilisation by autoclaving. Plates were then poured in a sterile environment and stored at 4$^{o}$C.

Antibiotics were commonly used at 1 in 1000 dilutions from stock solutions. Stocks were prepared: 100mg/ml ampicillin sodium salt in water, 50mg/ml Kanamycin sulphate in water.

2:2

General molecular biology methods

2:2:1

Agarose gel electrophoresis

Agarose powder (0.8 – 1.5% w/v) was dissolved in TAE buffer (40mM Tris-acetate, 1mM EDTA, pH8.0) by heating in a microwave. The solution was allowed to cool to around 50 degrees, before Ethidium Bromide (EtBr) was added to a final concentration 0.5 µg/ml. The solution was then allowed to cool completely and transferred to an electrophoresis tank containing TAE buffer. DNA samples were prepared for electrophoresis by the addition of 6x DNA loading buffer (40% (w/v) ficoll, 0.25% (w/v) bromophenol blue in water). Samples were then loaded into the gel alongside a 1kb or 100bp fragment marker. Gels were then run at 110 volts and DNA samples were then visualised using an ultraviolet transilluminator.

2:2:2

Mini DNA preparations

A single colony from a bacterial transformation was used to inoculate 5ml of 2YT containing appropriate selection agent. Cultures were grown overnight at 37$^{o}$C with shaking. Plasmid DNA was extracted using Promega Ltd Wizard Mini-prep kit following the manufacturer's instruction. 100µl sterile water was used to elute DNA from the column. Eluted DNA was stored at -20$^{o}$C.

2:2:3

Gel extraction / purification

Agarose gel electrophoresis was used to separate DNA by size. Bands of the correct size were identified using an ultraviolet transilluminator and excised from the gel using a scalpel and placed in a sterile 1.5ml Eppendorf tube. DNA was extracted from the gel using Qiagen QiaQuick Gel Extraction Kit as per the manufacturer's instructions

2:2:4

Restriction endonuclease digestion

Plasmid DNA was digested using 2 restriction endonucleases in the same buffer. Reactions were set up as follows:

| | |
|---|---|
| DNA / plasmid | 5 µg |
| 10 x buffer | 1 µl |
| Restriction enzyme #1 | 1 µl (20 units) |
| Restriction enzyme #2 | 1 µl (20 units) |
| Sterile water | Enough to make total volume 10µl |

2:2:5

Ligation reactions

Restriction digests of parent plasmid and desired insert were carried out as described above and isolated using gel extraction. Vector DNA was then treated with shrimp alkaline phosphatase SAP(15mins, 37$^{o}$C) to catalyse the dephosphorylation of the 5' phosphates and prevent vector re-ligation. SAP was then deactivated by heating to 65$^{o}$C for 15mins. Ligation reactions were set up on ice as follows:

| | |
|---|---|
| Vector DNA | 1 µg |
| Insert DNA | 3 µg |
| 10 x T4 DNA Ligase buffer | 1 µl |
| T4 DNA Ligase | 1 µl |
| Sterile water | Enough to make total volume 10µl |

Controls containing only vector DNA, only insert DNA and no DNA were included. Ligation reactions were carried out at 16$^{o}$C overnight and 10µl of the ligation reaction was transformed into Top10 cells and grown overnight on selective media as described in section 2.1.

2:2:6

Bacterial transformations

Chemically competent cells were thawed on ice for 15mins. 4µl of plasmid DNA (~1µg/µl) was added and incubated on ice for 15mins. Cells were then heat shocked at 42$^{o}$C for 1 minute before being returned to ice for 15mins. 250µl of SOC media was then added and cells were incubated for at least one hour 37$^{o}$C with shaking after which cells were spread out on plates containing appropriate antibiotics in a sterile environment, left to dry for 15mins and incubated overnight at 37$^{o}$C.

2:3

General protein methods

2:3:1

Expression of recombinant proteins

A single colony from a fresh transformation was picked and used to inoculate 2YT media (50-400ml) containing the appropriate antibiotic. Cultures were grown overnight at 37$^{o}$C with shaking and cells were collected by centrifugation at 1000 x g for 20mins. Cell pellet was then resuspended in Terrific Broth (10-50ml) containing appropriate antibiotic, this was then used to inoculate 1l of Terrific Broth. Cultures were grown at 37$^{o}$C with shaking to an optical density (OD) of 0.8. Recombinant protein expression was induced using 1mM Isopropyl-β-D-thiogalactopyranoside (IPTG) for 4hrs at 37$^{o}$C, or 1mM IPTG overnight at 22$^{o}$C. Cells were harvested by centrifugation at 3000 x g for 20mins after the induction period was complete.

2:3:2

Purification of $His_6$ tagged recombinant proteins

Cell pellets, collected as described above, were resuspended in cold phosphate buffered saline (PBS, 2.7 mM KCl, 1.8 mM $KH_2PO_4$, 137 mM NaCl, 10.1 mM $Na_2HPO_4$ )pH 7.4, Complete ™ protease inhibitor cocktail (Roche Diagnostics Ltd), and 25mM imidazole with a blender. Cell suspensions were then lysed using Microfluidizer M-110P cell disrupter set at 10,000 PSI. DNA was then digested by addition of DNAse I (10µg/µl) on ice for 30mins. Crude lysate was then cleared by centrifugation at 15,000rpm in a Beckman JA25.5 rotor for 45mins during which $Ni^{2+}$-NTA agarose beads were prepared by washing with lysis buffer. Cleared lysates were then incubated with $Ni^{2+}$NTA-agarose beads at 4°C overnight to allow $His_6$ tagged proteins to bind to the beads. Beads were harvested by pouring lysate through a Bio-Rad ECONO-Pac® disposable chromatography column. Collected beads were then washed with 5 column volumes of cold PBS pH7.4, Complete ™ protease inhibitor cocktail and 50mM imidazole. Recombinant protein was then eluted from the beads using cold PBS Complete ™ protease inhibitor cocktail and 400mM imidazole. 10 1ml elutions were taken from beads and frozen at -20°C.

2:3:3

Purification of GST-tagged recombinant proteins

Cell pellets were collected as described above and resuspended in cold PBS pH 7.4, Complete ™ protease inhibitor cocktail with a blender. Cells were lysed using Microfluidizer M-110Pset at 10,000 PSI. DNA was digested using DNAse I (1µg/µl) on ice for 30mins. a cleared lysate was then generated by centrifugation at 18,459 rcf using Beckman JA25.5 rotor during which time Glutathione sepharose 4B beads (GE healthcare Bio-sciences Ltd) were washed with cold PBS pH 7.4, containing complete ™ protease inhibitor cocktail. Lysate was then incubated overnight at 4°C to allow the GST-tagged protein to bind. Beads were harvested by pouring lysate through a Bio-Rad ECONO-Pac® disposable chromatography column. Collected beads were then washed with 5 column volumes of cold PBS pH7.4 containing 1% v/v Triton X-100, 5 column volumes of cold PBS pH7.4 containing 1M NaCl, and finally 5 column volumes PBS pH7.4. To remove protein from GST-tag and glutathione sepharose beads, beads were washed with thrombin cleavage buffer (50 mM Tris-HCl pH 8.0, 150 mM NaCl, 2.5 mM $CaCl_2$). Beads were then incubated with thrombin cleavage buffer containing 0.02units of thrombin (Sigma-Aldritch) per µl of sample for 2hrs at room temperature or overnight at 4°C.

2:3:4

Ion exchange chromatography

Anion exchange separations were carried out using on a MonoQ 5/50 column (GE healthcare Bio-sciences Ltd) buffer A (20mM Tris-HCl, pH 7.5 – 8.5) and buffer B (20mM Tris-HCl, pH 7.5-8.5 1M NaCl). The pH was adjusted to give better separation for proteins depending upon the isoelectric point (pI). Columns were connected to fast protein liquid chromatography (FPLC) system following manufacturers guidelines.

Purified recombinant protein samples were analysed using SDS-PAGE and Coomassie staining (described below) to determine fractions with the largest concentration of protein. These fractions were then pooled and dialysed into buffer 95% A, 5% buffer B. Protein samples were then filtered through 0.45µM syringe filter to remove any particulate matter which could block the column. The column was washed and equilibrated according to the manufactures guidelines (5 column volumes (CV) buffer A, 5CV buffer B, 5CV 95% buffer A 5% buffer B). Samples were loaded onto the column using a 5ml loop. To elute the protein a gradient of buffer B was run over the column from 5%-50% over 20CV. 1ml fractions were collected and samples matching absorbance peaks at A280 were analysed by SDS-PAGE and Coomassie staining to assess protein concentration and purity. Fractions containing protein of interest were pooled and concentrated before storage at -80$^{o}$C or immediately used in further experiments.

2:3:5

Concentrating protein samples

Protein samples were concentrated using Microcon centrifugation filtration units (Millipore, Livingstone UK). Appropriate molecular weight cut off was selected depending on the size of the protein of interest.

2:3:6

SDS PAGE

Polyacrylamide gel electrophoresis was used to resolve proteins. A 5% stacking gel was made using 30% acrylamide/bisacrylamide mixture (Anachem Ltd, Luton, Bedfordshire) in stacking buffer (25mM Tris-HCl pH6.8, 0.2% (w/v) SDS. Resolving gels were made between 7.5% and 15% depending upon size of the protein of interest in resolving buffer (75mM Tris-HCl pH 8.8, 0.2%(w/v) SDS). Gels were polymerized using ammonium persulfate and N, N,

N', N'- tetramethylenediamine. Gels were set up in Bio-Rad PROTEAN Tetra running apparatus and immersed in running buffer (25mM Tris base, 190mM glycine, 0.1%(w/v) SDS.

Protein samples were prepared by the addition of an equal volume 2x Laemmli sample buffer (LSB; 100mM Tris-HCl pH 6.8, 4% (w/v) SDS, 20% (v/v) glycerol, 0.2% (w/v) bromophenol blue, 10% (v/v) β- mercaptoethanol). Protein samples were loaded into wells in the stacking gel alongside prestained protein marker (New England Biolabs Inc, Hitchin, Herts) and run at a constant voltage of 80v through the stacking gel. This voltage was increased to 180v to move samples through the resolving gel.

2:3:7

Coomassie staining

Protein samples resolved using SDS PAGE were visualised by staining with Coomassie blue stain (0.25% (w/v) bromophenol blue in a solution of 45% methanol and 10% acetic acid (v/v)). Once prepared Coomassie blue stain was filtered through Whatman No 2 filter paper. SDS PAGE gels were stained for at least one hour after which gels were destained (10% methanol (v/v) and 5% (v/v)) to visualise bands of protein.

2:3:8

Western Blotting

SDS PAGE gels containing resolved protein samples were removed from glass plates and immersed in wet transfer buffer (25mM Tris base, 190mM glycine, 10% methanol (v/v)). Two sponges, two pieces of Whatman 3mm filter paper and one piece of nitrocellulose membrane was immersed in wet transfer buffer along with the gel. Using Bio-Rad Mini Trans-Blot Cell apparatus transfer cassettes were assembled according to the manufacturer's guidelines. Transfers were run at a constant current of 200mA for 2hrs or 40mA overnight.

2:3:9

Estimation of protein concentration

Bradford assays were performed as based on the method of Bradford to estimate the concentration of protein in samples. Standard curves were obtained using known concentrations of bovine serum albumin (BSA). All measurements were made using a spectrophotometer at 595nm.

2:3:10

Isothermal titration calorimetry

Protein-protein interactions were measured using isothermal titration calorimetry (ITC) on a MicroCal ITC200. Recombinant protein samples were dialysed into the same buffer over night at 4$^{o}$C. Blank titrations were carried out by titrating ligand into buffer alone. The result was then subtracted from each experiment. Results were analysed using the MicroCal Origin ITC software package to obtain binding enthalpy ($\Delta$H), the stoichiometry (*n*) and the association constant ($K_A$). A “one-set-of-sites” binding model was used which assumes that one or more ligands binds with similar affinities to a single site.

# 3

# Results and Discussion

## 3:1

## Production of recombinant SNARE proteins

### Introduction

The aim of this project was to assess the binding kinetics of SNARE proteins involved in GLUT4 vesicle fusion with the plasma membrane in insulin responsive cells. To investigate the binding of SNARE proteins in further detail it was necessary to produce each of the SNARE proteins in a recombinant system. All recombinant proteins were derived from mouse cDNA and all constructs with the exception of the GST tagged Munc18c construct pGEXM18c were produced by previous students. Many of the constructs which were previously made had undergone some level of optimisation for use in other assays by other students. To allow ITC experiments to be carried out further optimisation was required on all proteins to increase purity and remove contaminating nucleotides whilst still maintaining protein concentrations within a useable range for experimentation.

Initial work was carried out using syntaxin 4 – ΔTMD (syntaxin 4 with transmembrane domain removed), SNAP23 and VAMP2. These proteins were produced using two different purification systems with SNAP23 being $His_6$ tagged and syntaxin 4 – ΔTMD and VAMP2 being GST tagged.

## 3:2

### Syntaxin 4 ΔTMD – GST and Syntaxin 4 ΔTMD L173A E174A - GST purification

A syntaxin 4 construct was produced lacking the C terminal transmembrane domain (TMD) using pGEX 4T vector (GE Healthcare) in a similar way to Fasshaeur et al (Fasshaeur et al 1999) The TMD was removed to increase the solubility of syntaxin 4 and allow ITC experiments to be carried out without the need for detergent to solubilise the protein. Syntaxin 4 ΔTMD –GST was produced as described in the methods section 2:3:3. Typically 6-12l of bacterial culture was produced to give sufficient protein concentration after

purification. After cleavage of the GST tag using thrombin, eluted protein was visualised using SDS PAGE and Coomassie staining as described in the methods section of this report. Fig 10 shows a typical syntaxin 4 ΔTMD-GST recombinant protein preparation.

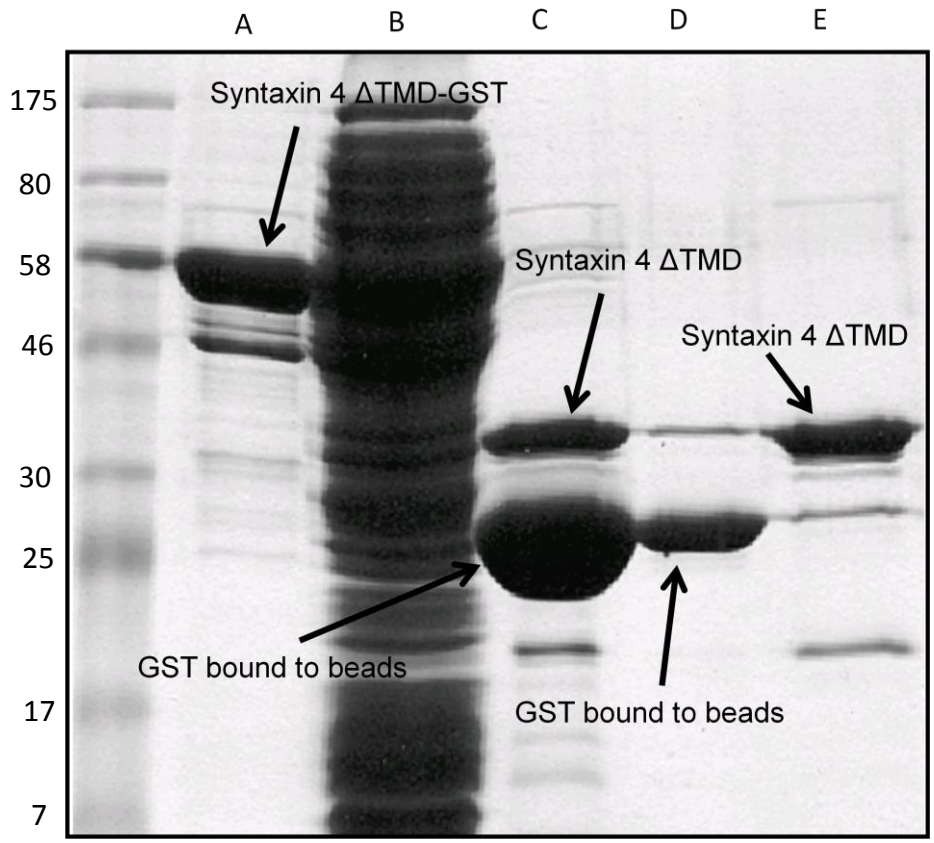


***Figure 10**, pGEX vector containing mouse syntaxin 4 lacking the transmembrane domain was expressed in BL21 cells and purified using glutathione sepharose beads. Proteins were separated using SDS PAGE. Gel was stained with Coomassie blue: (A) Glutathione sepharose beads bound to syntaxin 4 ΔTMD-GST. (B) BL21 bacterial lysate after overnight incubation with glutathione sepharose beads. (C) Glutathione sepharose beads after 4hours proteolytic thrombin cleavage showing GST bound beads and free syntaxin 4 ΔTMD. (D) Glutathione sepharose beads bound to cleaved GST after elution of solubilised syntaxin 4 ΔTMD. (E) Soluble syntaxin 4 ΔTMD eluted from beads. Multiple bands are likely to be un bound GST, GST bound to beads and proteolytic cleavage products of syntaxin 4 ΔTMD*

The purified syntaxin 4 ΔTMD seen in lane E of figure 10 has multiple visible protein bands. For use in ITC experiments a single band is preferable for each input sample. Therefore the protein purification protocol was optimised to reduce and remove contaminant bands. Ion exchange chromatography was used to further purify samples of recombinant protein and has been used to purify neuronal SNARE proteins by Fasshauer et al (Fasshauer et al 1999). Ion exchange chromatography allows for the separation of proteins based upon their

charge. The theoretical pI of mouse syntaxin 4 ΔTMD was obtained using the ProtParam tool using the correct nucleotide sequence which lacks the transmembrane domain. As the pI was below 7.4, Tris buffer was used at pH 8.1 allowing syntaxin 4 ΔTMD to maintain a positive charge allowing it to bind to MonoQ beads which carry a strong anion charge. Figure 12 shows an SDS PAGE containing samples taken from fractions containing peaks of absorbance shown in figure 11.

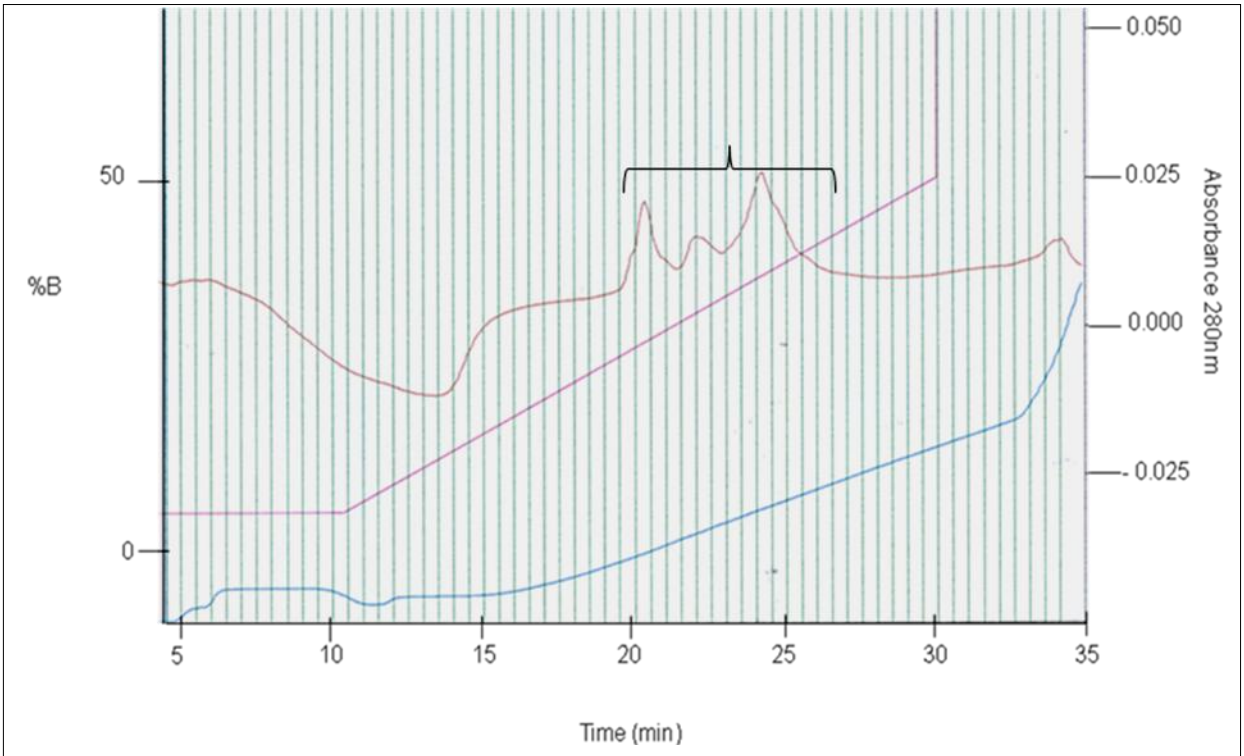


***Figure 11.*** *Graph showing absorbance, percentage of buffer B (eluent), and conductivity of syntaxin 4 ΔTMD recombinant protein sample ion exchange chromatography. The graph shows absorbance measured at 280nm in red, percentage of buffer B flowing through the column in pink, and conductivity in blue. Fractions were collected automatically as indicated by the vertical green lines. The samples included in the parenthesis were analysed by SDS PAGE and stained using Coomassie blue to visualise proteins.*

Figure 11 shows three distinct peaks in absorbance at 280nm between 20 and 27mins. These peaks correspond to protein eluting from the column as an increasing concentration of NaCl flows through the column. Samples from the fractions within these peaks were analysed using SDS PAGE and proteins visualised by staining with Coomassie blue. Figure 12 shows the proteins separated using ion exchange chromatography from the recombinant

syntaxin 4 ΔTMD protein. It is apparent that syntaxin 4 ΔTMD was eluted primarily in the first peak without any other contaminating bands. As the NaCl concentration increased the lower molecular weight proteins were eluted, the protein at 30Kd being eluted with some recombinant syntaxin 4 ΔTMD followed by the protein at 25kd and subsequently followed by the lowest visible contaminating protein at 18kd.

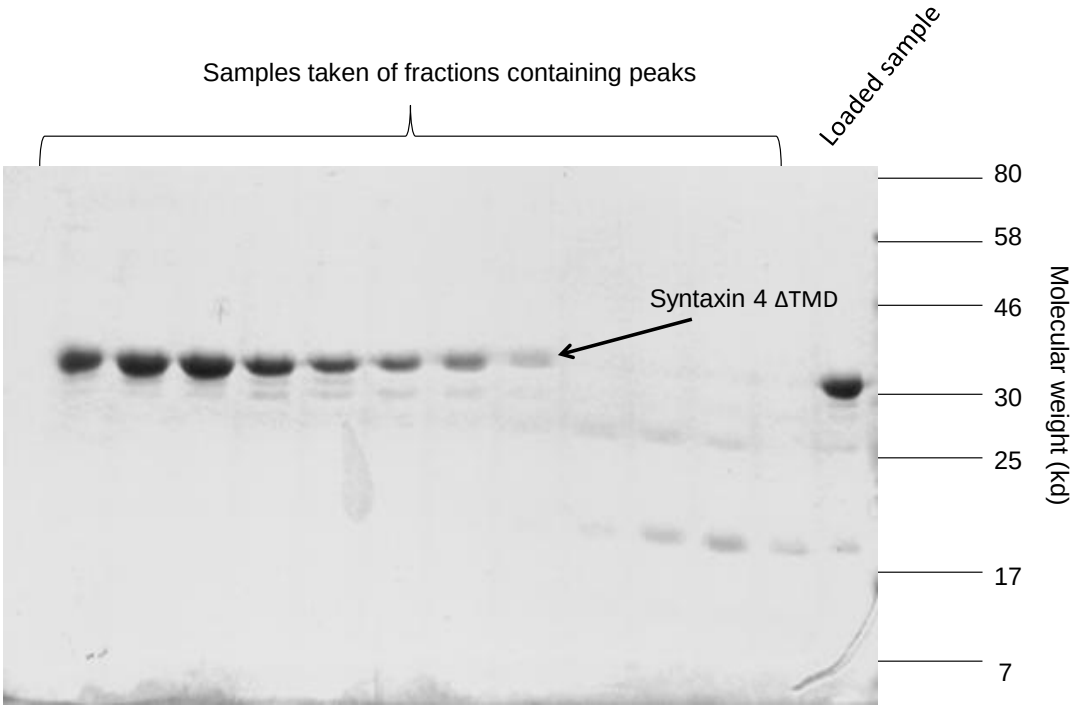


***Figure 12*** *Syntaxin4-GST recombinant protein ion exchange profile. Buffer conditions: Solvent buffer 20mM tris pH 8.1, Eluent buffer same as solvent with the addition of 0.5M NaCl. SDS-PAGE was used to separate samples of syntaxin 4 ΔTMD protein fractions after ion exchange using a MonoQ column. Gel was stained with Coomassie. Samples were taken from fractions containing peaks as shown in figure 11. 10µl of each fraction was loaded.*

Although the purity of syntaxin 4 ΔTMD recombinant protein production using a GST tag system was improved using ion exchange chromatography this process increased the amount of time taken to produce a usable protein sample. The increase in time spent at room temperature or 4$^{o}$C as protein samples needed to be dialysed into the correct buffer overnight and the ion exchange chromatography itself was carried out at room temperature made the protein liable to degrade before use. The ion exchange chromatography process also decreased the concentration of syntaxin 4 ΔTMD in solution due to the syntaxin 4

ΔTMD eluting from the column over several fractions with only some eluting without other contaminating proteins.

Therefore, rather than implementing ion exchange chromatography as part of the recombinant protein production for syntaxin 4 ΔTMD constructs, instead the recombinant protein purification itself would be improved to increase the purity of sample, decrease the length of time for protein production and still maintain high concentrations of protein. This protocol for GST protein production is described in this report. A Biorad® Econo-Pac disposable column system was used to collect all glutathione sepharose beads added into cleared bacterial lysate. This allowed for more thorough washes and a decrease in amount of beads lost compared to previous protocols whereby beads were collected by centrifugation. The wash steps themselves were also modified, a Triton X-100 wash step was used to remove bound hydrophobic proteins, and an increased concentration of NaCl in a high salt wash step was used to remove ionic bound proteins. Both volume and number of washes was increased to remove as much protein contamination as possible.

Figure 13 shows syntaxin 4 ΔTMD recombinant protein purification produced using modified protocol, proteins were analysed using SDS-PAGE and stained using Coomassie blue to visualise. This figure shows fewer contaminants in the final lane (syntaxin 4 ΔTMD) and therefore it was deemed unnecessary to use ion exchange chromatography to further purify this protein.

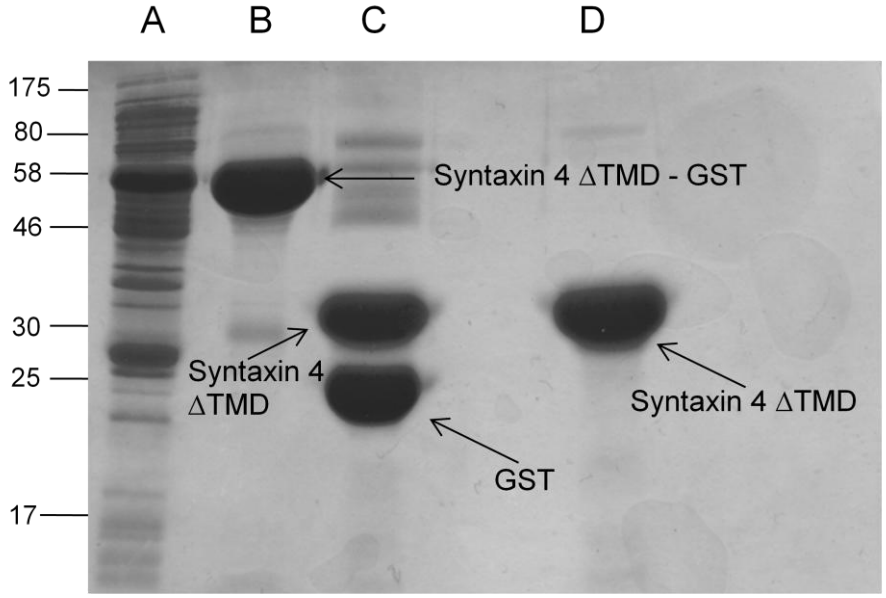


**Figure 13** *pGEX vector containing wildtype mouse syntaxin 4 ΔTMD was expressed in BL21 cells and purified using glutathione sepharose beads. Proteins were separated using SDS-PAGE and stained with Coomassie blue: (A) BL21 cell lysate after overnight incubation with Glutathione Sepharose beads. (B) Isolated Glutathione beads bound to syntaxin 4*

*ΔTMD GST. (C) Glutathione Sepharose beads after 4hours proteolytic thrombin cleavage showing GST bound to glutathione beads and free syntaxin 4 ΔTMD. (D) Soluble syntaxin 4 ΔTMD eluted from beads*.

The constitutively open mutant of syntaxin 4 has been described previously (D'Andrea-Merrins et al 2007) (Arran et al) and was initially created by mutating the highly conserved homologous amino acids from syntaxin 1a (Sudorf & Rizo et al 1999) and has been validated by comparison to the homologous mutation in syntaxin 1a (Richmond L. E. et al 2001). The constitutively open mutant was produced using the same protocol as for wild type syntaxin 4 ΔTMD. Figure 14 shows a typical purification of syntaxin 4 ΔTMD L173A E174A protein.

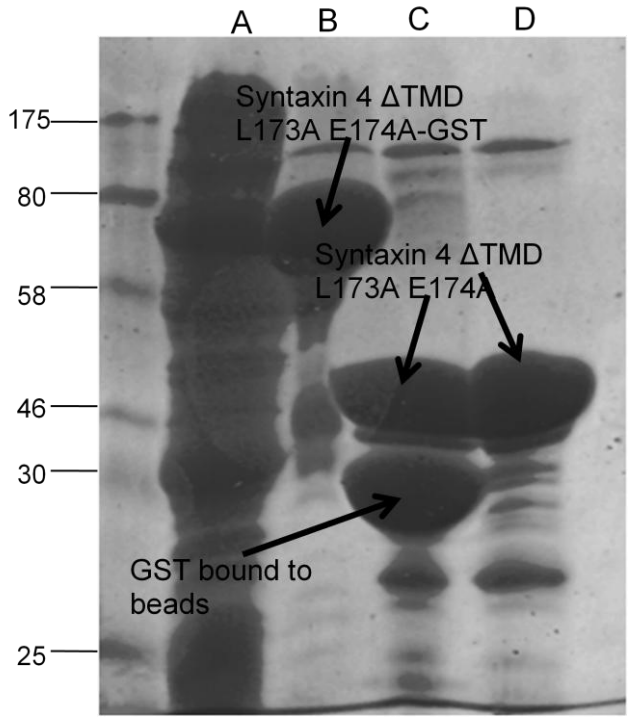


**Figure 14** *pGEX vector containing mouse constitutively open conformation syntaxin 4 ΔTMD L173A E174A was expressed in BL21 cells and purified using glutathione sepharose beads. Proteins were separated using SDS-PAGE and stained with Coomassie blue: (A) BL21 cell lysate after overnight incubation with Glutathione sepharose beads. (B) Isolated Glutathione sepharose beads bound to syntaxin 4 ΔTMD L173A E174A- GST. (C) Glutathione sepharose beads after 4hours proteolytic thrombin cleavage showing GST bound to glutathione beads and free syntaxin 4 ΔTMD L173A E174A. (D) Soluble syntaxin 4 ΔTMD L173A E174A eluted from beads. Gel has been overloaded with protein causing distortion of bands. Bands of interest are labeled accordingly*

3:3

Wild type SNAP23 $His_6$ tagged protein purification.

A construct was created by a previous student using wild type SNAP23 in a pQE-30 vector (Qiagen, Crawley, West Sussex, UK) to generate a $His_6$ tagged protein as described by Terpe (Terpe K. 2003). This same vector and purification system has been used previously for SNARE and SM protein purification (Barclay J. W et al 2003). SNAP23 has no transmembrane domain but is rather held in the plasma membrane by palmitoylated sites in the flexible linker region between the two SNARE domains; recombinant SNAP23 therefore is soluble as a full length protein. While it is possible to produce constructs where the His tag is cleavable, this was deemed unnecessary for use in this project so no cleavage of the protein was carried out. Purification was carried out according to section 2:3:2 using $Ni^{2+}$-NTA agarose beads. Using a $His_6$ - $Ni^{2+}$-NTA affinity system was deemed necessary as previous work done by other students using GST-SNAP23 showed low levels of protein production after purification, and cleavage of the large GST tag was also ineffective (unpublished work).

Using protocols designed by previous students frequently resulted in contaminating proteins which were eluted from $Ni^{2+}$-NTA agarose beads along with recombinant SNAP23. Figure 14 shows a typical SNAP23 protein elution from $Ni^{2+}$-NTA agarose beads using such a protocol.

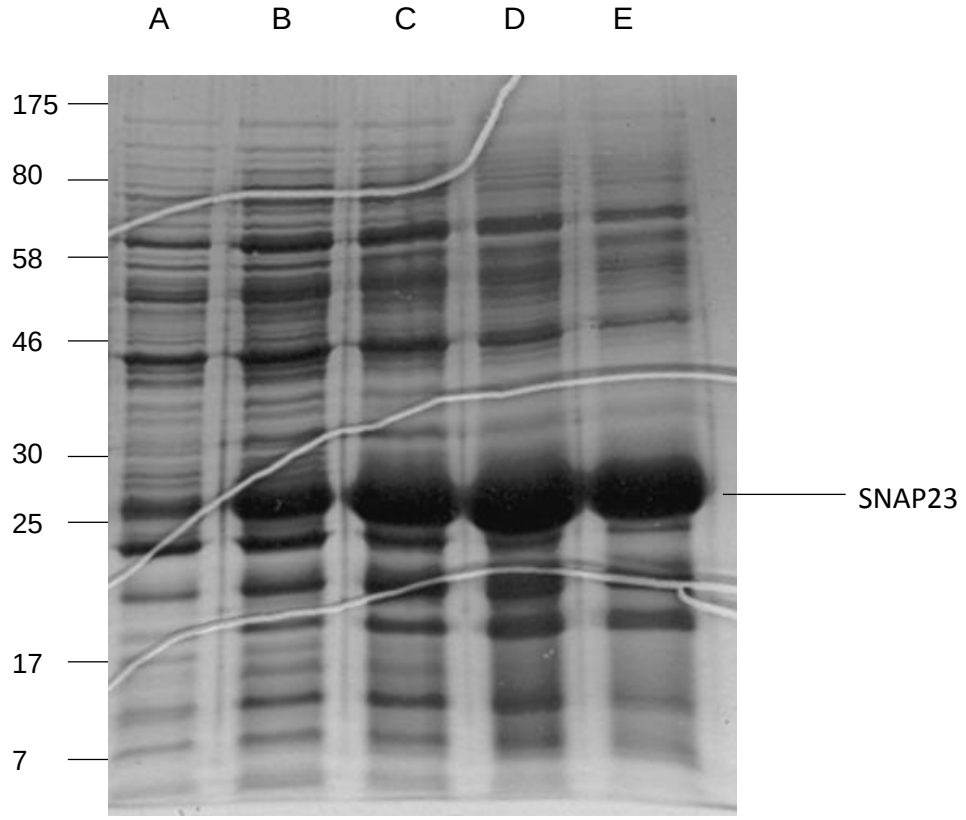


***Figure 14**. pQE-30 vector containing wildtype mouse SNAP23 was expressed in BL21 cells and purified using $Ni^{2+}$ - NTA agarose beads. SDS-PAGE was use to separate proteins. Gel was stained with Coomassie blue showing 5 elutions of $His_6$ – SNAP23: (A) elution with 50mM imidazole, (B) elution with 100mM imidazole, (C) elution with 150mM imidazole, (D) elution with 200mM imidazole, (E) elution with 250mM imidazole*

The purity of SNAP23 in the eluted samples shown in figure 14 was too low for use in ITC experiments. To improve purity the protocol was modified to decrease the amount of non specific binding of bacterial proteins from the cleared bacterial lysate to the $Ni^{2+}$-NTA agarose beads. Firstly a low concentration of imidazole (25mM) was included in the lysis buffer during incubation with $Ni^{2+}$- NTA beads to decrease non-specific binding (Terpe K. 2003). After incubation with beads the number and volume of washes with PBS was increased with the inclusion of 50mM imidazole to further remove non specific bound proteins. To improve the elution step the concentration of imidazole was increased to 400mM over a larger number of fractions all of which were then analysed by SDS-PAGE and stained using Coomassie blue. This allowed identification of fractions containing the highest purity and the highest concentration. Multiple elution fractions were then pooled and concentrated as described in section 2:3:5 before use in ITC experiments. Figure 15 shows

improved purity of SNAP23 using this modified protocol, far fewer contaminating proteins are observed.

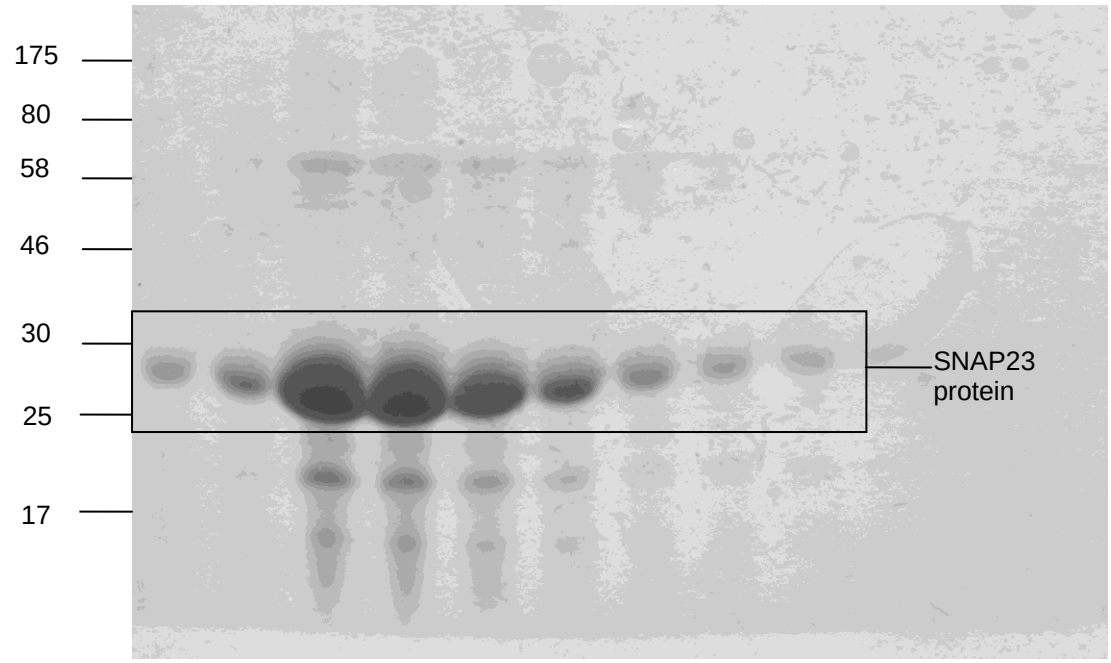


***Figure 15*** *pQE-30 vector containing mouse SNAP23 was expressed in BL21 cells and purified using $Ni^{2+}$-NTA Agarose beads. Proteins were separated using SDS-PAGE and stained with Coomassie blue. Gel shows samples from 1ml elutions of SNAP23 from Ni-Agarose beads with 400mm imidazole in PBS*

3:4

Wildtype VAMP2 recombinant protein purification.

A VAMP2 construct was produced by D. Kioumourtzoglou (unpublished work) lacking the C terminal transmembrane domain (TMD) using pGEX 4T vector (GE Healthcare). The TMD was removed to increase the solubility and allow ITC experiments to be carried out without the need for detergent or lipid membranes to solubilise the protein. VAMP2 was produced using the same modified protocols established for syntaxin4 which eliminated the need for ion exchange chromatography. Figure 16 shows a typical VAMP2 ΔTMD recombinant protein purification.

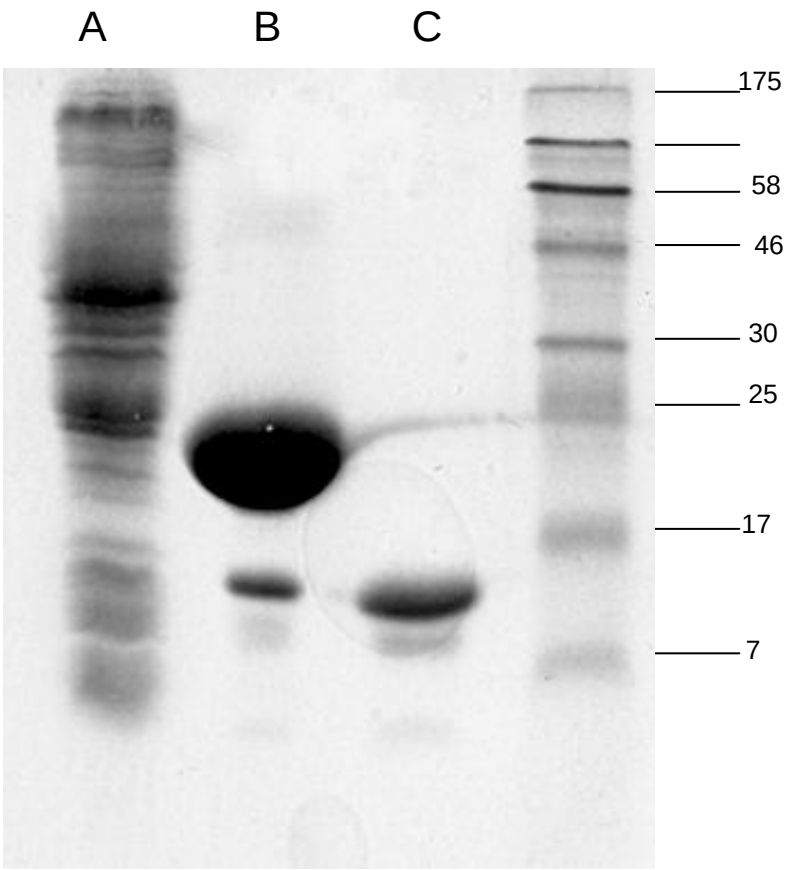


***Figure 16*** *pGEX 4T vector containing VAMP2 ΔTMD was expressed in BL21 cells and purified using glutathione sepharose beads. SDS-PAGE was used to separate proteins which were then stained with Coomassie blue. Gel shows samples of: (A) BL21 cell lysate after overnight incubation with Glutathione Sepharose beads. (B) Glutathione sepharose beads after 4hours proteolytic thrombin cleavage showing GST bound to glutathione beads and soluble VAMP2. (D) Soluble WT VAMP2 ΔTMD eluted from beads*

3:5

Munc18c protein purification

A construct was created by a current student using pET28b vector containing wild type Munc18c to generate N-terminally $His_6$ tagged Munc18c. This was then purified using $Ni^{2+}$-NTA agarose beads using the same protocol established for SNAP23 (Terpe K. 2003). Figure 17 shows a typical Munc18c-$His_6$ recombinant protein purification, showing elutions from $Ni^{2+}$-NTA agarose beads using an increasing concentration of imidazole. There were multiple bands present in each sample which were visualised after staining with Coomassie blue. To improve purity ion exchange chromatography was used using a cation exchange MonoS column, replicating Wiederhold and Fasshauer (Wiederhold and Fasshauer 2009), using buffers at pH 7.4 appropriate for Munc18c which has a theoretical isoelectric point of 8.28. However there was no separation of Munc18c from contaminant proteins and the levels of Munc18c produced were too low for this to be a viable option for protein production. For use in ITC higher levels of purity and concentration of protein were needed than obtained using the $His_6$ - $Ni^{2+}$-NTA agarose system therefore a new construct was created using a pGEX vector to create thrombin cleavable GST tagged Munc18c similar to D'Andrea-Merrins et al (D'Andrea-Merrins 2007). This construct was created to provide similar levels of protein as the VAMP2 and syntaxin4 constructs which were both created using the pGEX system and both showed consistently higher levels of protein when compared to Munc18c pET28b construct. Using the pGEX system also allows the cleavage of the GST tag from the protein of interest. This should also improve purity and final concentration. Using the pGEX system also reduces variability between constructs.

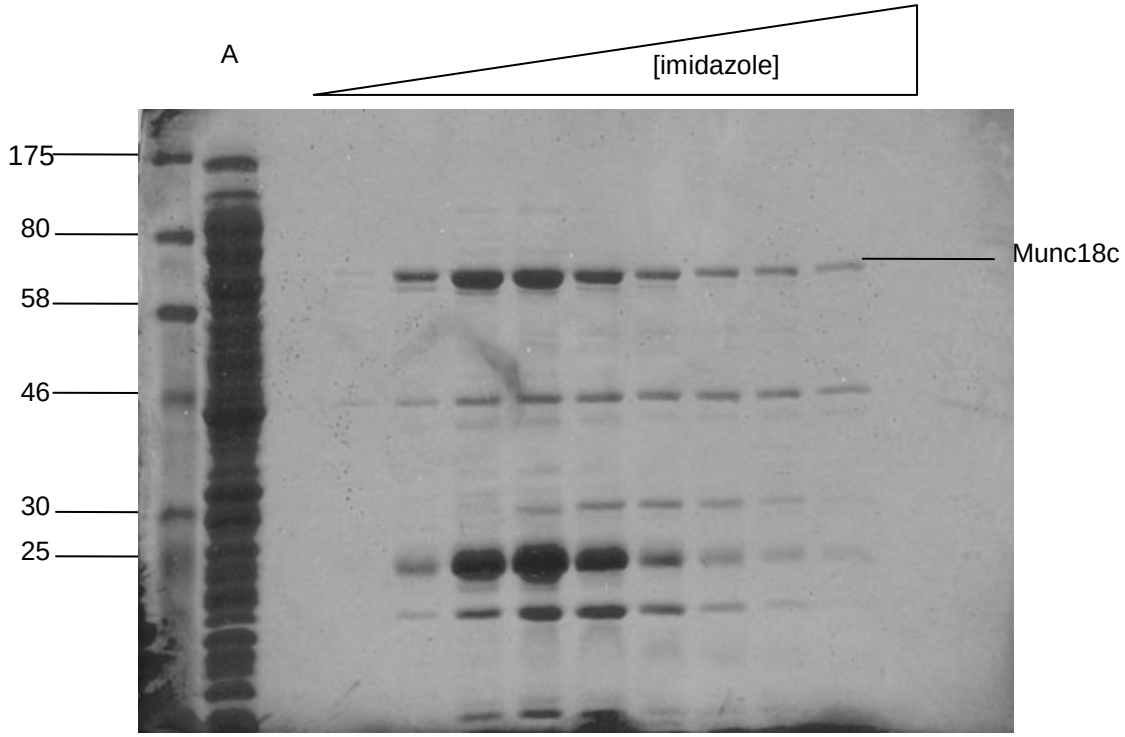


***Figure 17*** *pET28b vector containing Munc18c was expressed in BL21 cells and purified using Ni-Agarose beads. Proteins were separated using SDS-PAGE and stained with Coomassie blue. Gel shows samples from: BL21 bacterial cell lysate (A). 1ml elutions of* $His_6$*-Munc18c from Ni-Agarose beads over an increasing gradient of imidazole in PBS*

3:5:1

Production of Munc18c – GST in pGEX vector.

In an effort to create a GST tagged Munc18c protein similar to D'Andrea-Mellins et al (D'Andrea-Mellins et al 2007) the same pGEX-4T vector as VAMP2 and syntaxin4 constructs a Munc18c –GST vector was created. The Munc18c fragment was excised from pET28b according to the protocol outlined in section 2:3:3 using BamHI and XhoI. Empty pGEX 4t vector was digested using the same enzymes to allow ligation and insertion of Munc18c construct. Successful transformats were screened for correct insertion. Samples that showed successful ligation were re-transformed into BL21 *E.coli* cells for recombinant protein purification according to the protocols outlined in section 2:2:5. Munc18c – GST was purified using the same techniques described for syntaxin4 and VAMP2. Samples of cleaved Munc18c were analysed using SDS-PAGE and visualised using Coomassie stain. Figure 18 shows a typical recombinant protein purification of Munc18c-GST.

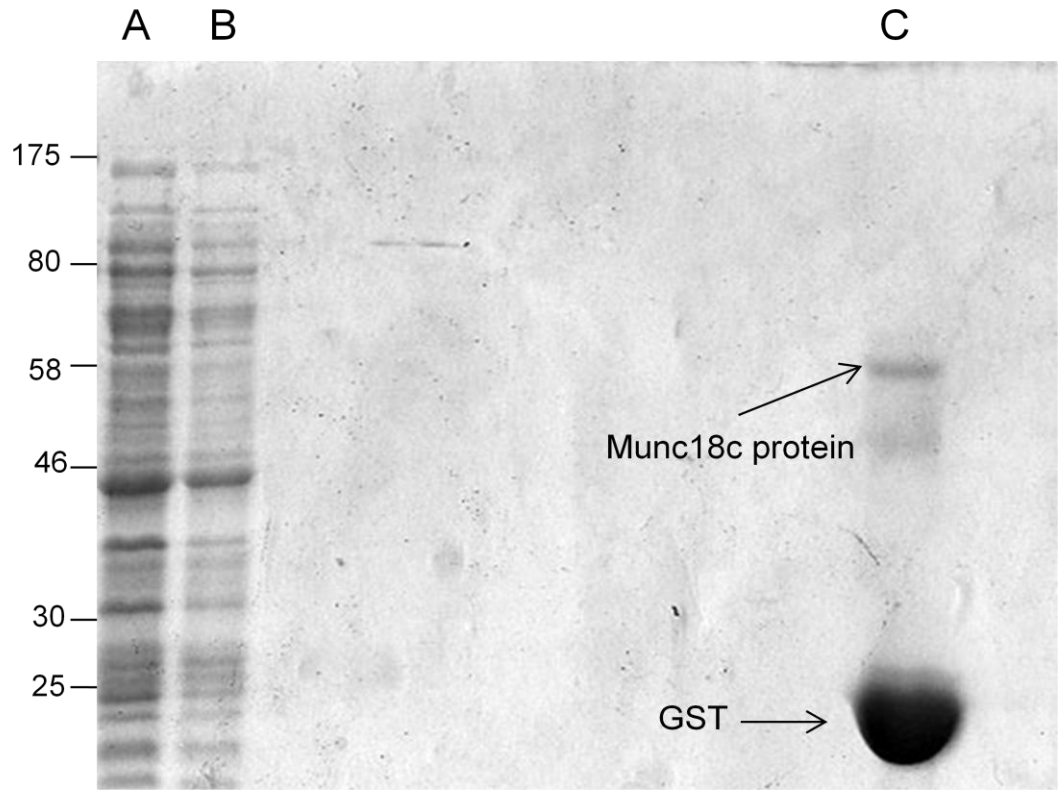


***Figure 18*** *pGEX-4T vector containing Munc18c was expressed in BL21 cells and purified using glutathione sepharose beads. Proteins were separated using SDS-PAGE and stained with Coomassie blue. Gel shows: A) and B) samples of PBS washes of glutathione beads, C) Elution from beads after 4hours proteolytic thrombin cleavage showing GST bound to glutathione beads and free Munc18c*

As can be seen in figure 18, overall concentration of the Munc18c – GST fusion protein was very low. In comparison to other protein produced using the same pGEX – 4T vector, the levels of protein both bound to the beads and especially the levels of protein after cleavage were much lower. The general protocol developed for syntaxin4 and VAMP2-GST protein purification detailed in section 2:3:3 was then modified to try to improve efficiency and quantity of protein production. Larger quantities of thrombin were added and cleavage was carried out overnight at 4$^{o}$C to try to improve yields. While purity of the protein was greatly improved with only one visible band, the efficiency was greatly decreased with very low amounts of protein produced per litre of bacterial culture. Protein production using the generated Munc18c-GST construct needed more optimisation than the time scale of this project would allow, therefore ITC experiments were carried out using the Munc18c – $His_6$ construct.

3:6

Protein purification discussion

In general terms the purification steps described above were the result of extensive work on the optimisation of manufacturers' protocols and protocols already set up by previous members of the research group (Arran et al). It was the efforts of this project that allowed highly pure and concentrated samples to be produced using new systems and more rigorous quality control.

Specifically for each protein it was necessary to test the following parameters before being used for ITC experiments: Total volume of bacterial growth media to provide enough recombinant protein, duration of induction with IPTG in culture, volume of lysis buffer and subsequent volume of beads for purification, length of incubation with beads and temperature of incubation, collection of maximum amount of beads, washing of beads to remove contaminants, elution of protein from beads before enzymatic cleavage, concentration of thrombin for enzymatic cleavage, concentration of target protein, levels of residual contamination in final protein sample. This list does not take into account the development of ion-exchange chromatography as a means to increase protein purity which has its own level of optimisation to take into account including: theoretical PI of each protein, use of correct buffer to maintain PI and solubility of protein, equilibration of column prior to sample loading, correct length of time to bind sample to column, duration of column washing, duration of sample elution, volume of each fraction to be collected, assessment of each peak fraction for protein level.

Each of these parameters was considered and steps were taken to ensure the highest possible purity and highest possible quantity of protein was produced. The difficulty was getting both these aspects together; it was possible to produce Munc18c for example at a high purity using a GST construct. However the concentration of this protein was very low in the final sample. If the His tagged construct was used the purity was much reduced with contaminating bands always present but the concentration of protein in the final sample was much greater. This is indicative of the production of the different proteins in this project. Whilst improvements were made in the production which are detailed above, these improvements took a very large amount of time as each step of the process was highly labour and time intensive. It was also very difficult to produce a large quantity of multiple proteins at the same time, as often each protein would require around 10 litres of bacterial broth. This led to further problem of storage of proteins after they were produced, as some did not stay in solution after freeze thaw cycles whilst others would degrade when left at $4^{o}$C.

The length of time it took to optimise each step of the protein purification decreased the amount of time needed to optimise the ITC experiments. As a result only a small number of ITC experiments were performed not all of which produced useful data. These are further discussed below in section 3:7

3:7

ITC analysis of syntaxin 4 – ΔTMD, syntaxin 4 ΔTMD- L173A E174A, SNAP23 and Munc18c binding kinetics.

To establish the assay we first set out to obtain the affinity of SNAP23 for syntaxin4 – ΔTMD. The interaction between these two proteins is well described (Ravichandran V., et al 1996; Foster L. J. 1998). Both these proteins were produced using a recombinant protein production system as described above. Initial experiments showed a large enthalpic change upon the injection of SNAP23 into buffer alone as shown in figure 20. This step is done to establish a baseline for comparison when injecting into the second protein. The large positive enthalpy, demonstrated by a negative energy reading on the y axis, is an unexpected result and is most commonly caused by a mismatch in buffer between the syringe and cell. However syntaxin 4 ΔTMD and SNAP23 were dialysed in the same buffer before each experiment and the same result was not seen upon injection of syntaxin4 – ΔTMD into buffer alone so a mismatch of buffers seems an unlikely explanation. Another possibility is that a change in conformation of SNAP23 after injection into the cell caused a change in enthalpy which was measurable. SNAP23 contains two SNARE domains joined by a flexible peptide change which bind to one another to form a more stable closed conformation. Due to the design of ITC experiments proteins are titrated from a high concentration in the syringe into a cell containing only buffer. This sudden change in concentration could change the conformation of SNAP23 which could have given the observed large enthalpy change. SNAP23 could also have been more stable at high concentrations forming homodimers with two SNAP23 molecules forming a 4 helix SNARE bundle similar to the ternary SNARE complex. When diluted upon injection there could have been a shift to the endogenous monomeric SNAP23 conformation which also could have given rise to an observable enthalpy change. These hypotheses would require much further testing but the generation of a SNAP23 construct in which the SNARE domains were unable to bind to each other, similar to the constitutively open syntaxin 4 mutant, could possibly provide an explanation.

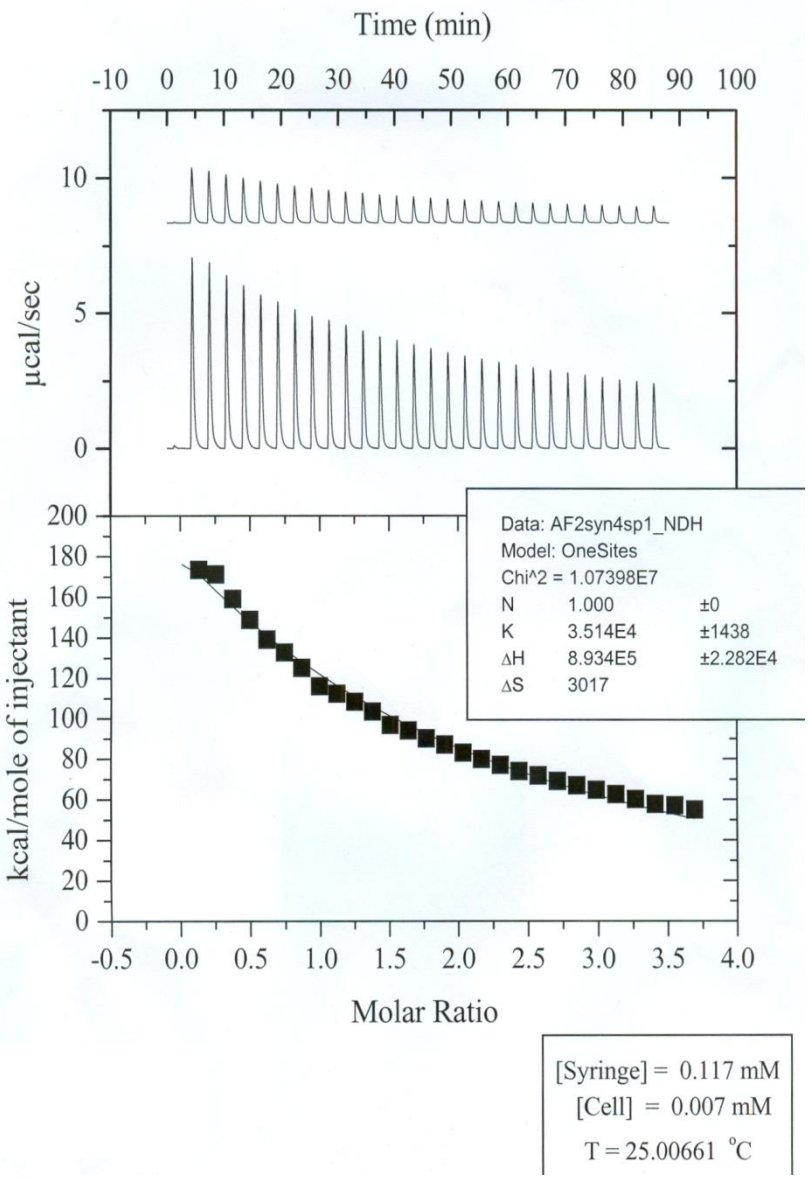


***Figure 19.*** *ITC experiments were performed at 25 °C in PBS, pH 7.4.The top panel shows the raw data in power versus time during the injections of syntaxin 4ΔTMD into the cell containing buffer alone (top graph), and then a cell containing SNAP23 (second graph). The lower panel displays the integrated areas normalized to the amount of the injectant (kcal mol$^{-1}$) versus its molar ratio to the protein in the cell. The solid lines represent the best fit to the data using a nonlinear least squares fit using a one-set-of-sites model. The highest concentrations obtainable were used for both proteins within the cell and syringe shown in figure*

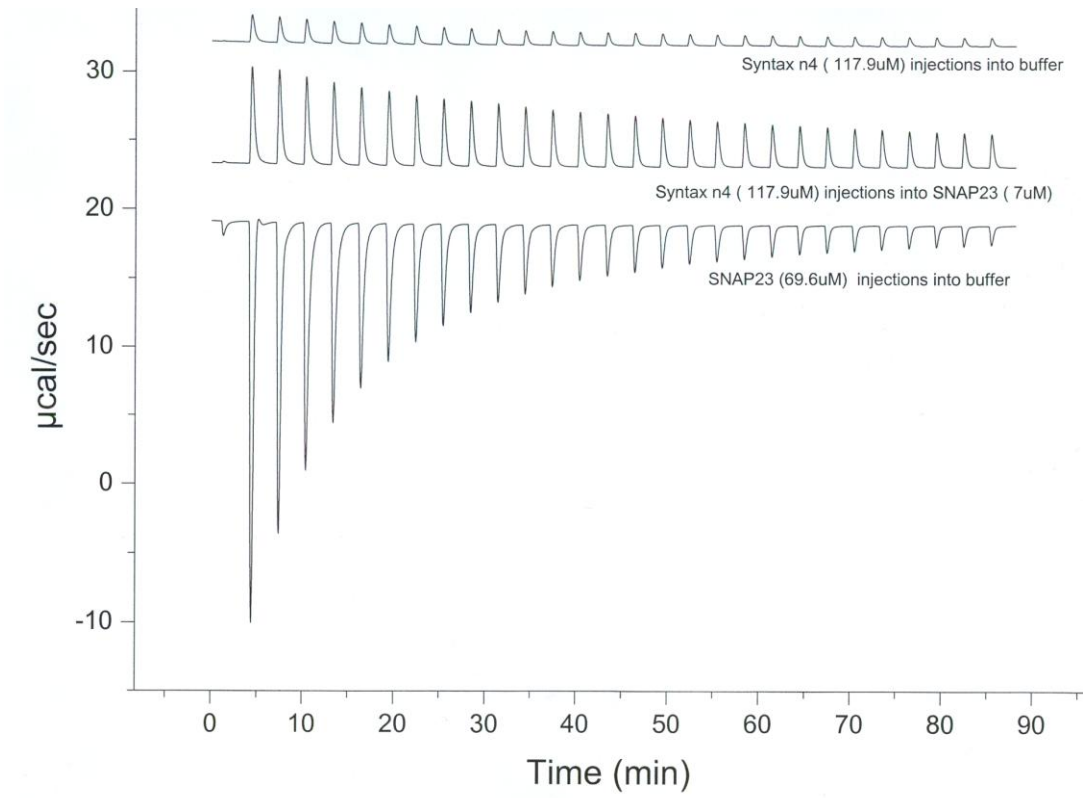


***Figure 20*** *ITC experiments were performed at 25 °C in PBS, pH 7.4.The top graph shows the raw data in power versus time during the injections of syntaxin 4ΔTMD into the cell containing buffer alone (top graph), a cell containing SNAP23 (second graph), and injections of SNAP23 into buffer alone (bottom graph).Top and middle graph can be seen alone in figure 19. Concentrations of each protein are labeled under each graph.*

The titration of syntaxin4-ΔTMD domain into a cell containing SNAP23 gave a different result when compared to the titration of SNAP23 into a cell containing syntaxin 4- ΔTMD. Upon injection of syntaxin4-ΔTMD into SNAP23 a negative enthalpy change was observed. This diminished as more syntaxin 4 ΔTMD was titrated into the cell containing SNAP23, however there continued to be enthalpy changes observed up until the final injection which suggests that the reaction was not saturated as shown in figure 19. Interestingly the titration of syntaxin 4- ΔTMD into buffer alone showed a much reduced enthalpy change unlike the titration of SNAP23 into buffer. Even without the titrations reaching the established baseline the results suggest an interaction between the two proteins. However when this result is compared to previously generated data by other laboratories (Wiederhold and Fasshauer

2009) the outcome is very different. The enthalpy change observed by the interactions of other SNARE proteins is the opposite of the change observed in this project. There are crucial differences between the experiments: firstly the use of the neuronal SNARE proteins syntaxin 1a, SNAP25 and VAMP1, secondly only the SNARE domain of syntaxin 1a was used as Wiederhold and Fasshauer were not looking at Munc18c interactions (Wiederhold and Fasshauer 2009). The core SNARE domains share a large amount of similarity which would be expected to produce similar results.

The interaction between syntaxin 4 ΔTMD and Munc18c was also assessed using ITC and gave similar results to the interaction of syntaxin 4-ΔTMD and SNAP23. A measurable negative enthalpy change was observed upon the injection of syntaxin 4 ΔTMD into buffer alone to establish a baseline similar to that observed in figure 19. When the data was normalized against the results of titrations of syntaxin 4 ΔTMD into Munc18c no model could be fitted to the data to generate K, $\Delta$H or $\Delta$S values. The raw data from this experiment is shown in figure 21. This suggests no observable interaction of the two proteins within the confines of this experiment. As syntaxin 4 ΔTMD and Munc18c have been shown previously to interact (D'Andrea-Merrins et al 2007) the ITC experiment was considered unsuccessful.

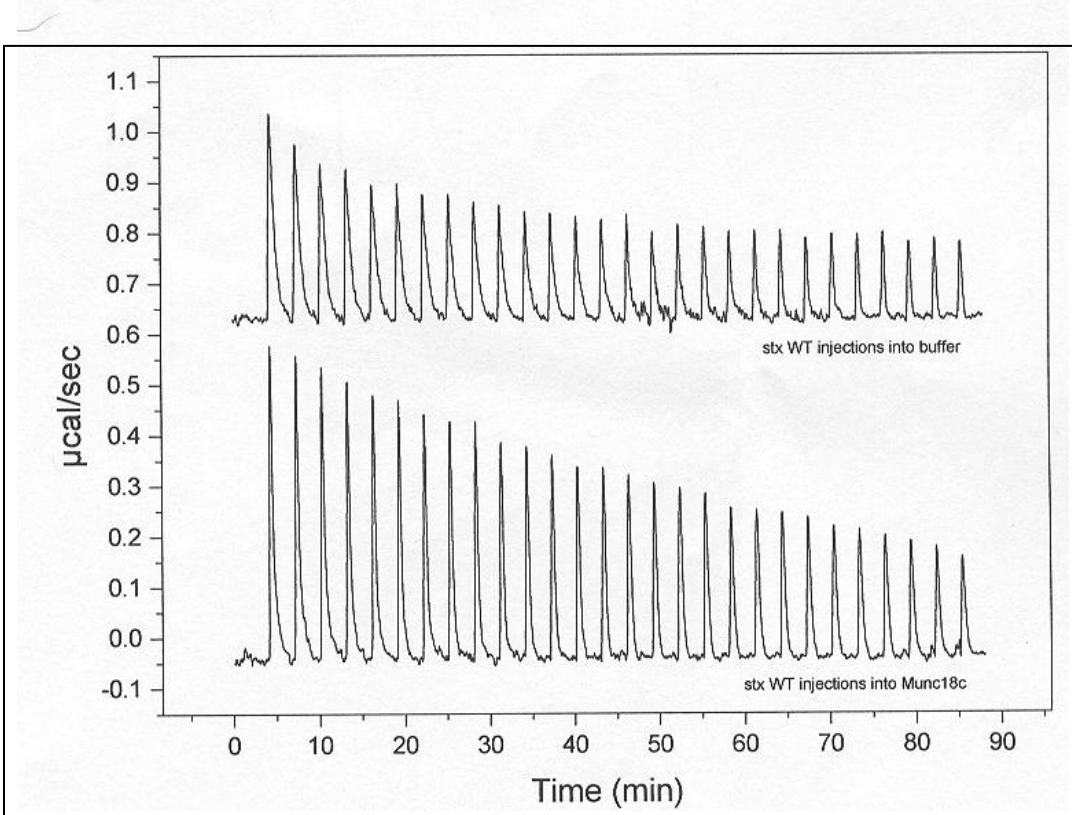


***Figure 21*** *All ITC experiments were performed at 25 °C in PBS, pH 7.4. In A), the top panel shows the raw data in power versus time during the injections of syntaxin 4 ΔTMD into a cell containing buffer alone. Observable enthalpy changes are similar to previous experiments (figure 19). The lower panel shows the raw data in power versus time during the injections of syntaxin 4 ΔTMD into a cell containing Munc18c. Once this data was normalized by taking into account the control experiment shown in the top graph, no model could be fitted to give K, ΔH or ΔS values.*

The Munc18c - syntaxin 4 ΔTMD interaction was further assessed by using a syntaxin 4 ΔTMD- L173A E174A mutant which has a constitutively open $H_{abc}$ domain. This was performed to elucidate the difference between the binding modes of syntaxin 4 ΔTMD N terminal domain with the hydrophobic pocket of Munc18c, and the binding of Munc18c to the closed form of syntaxin 4 ΔTMD. We also hypothesised that by using the constitutively open form of syntaxin 4 we could decrease the enthalpy change when titrating only syntaxin 4 into buffer as this enthalpy change could be attributed to the endongenous binding of the syntaxin $H_{abc}$ domain to the SNARE domain. When syntaxin 4 ΔTMD- L173A E174A was injected into buffer alone an observable positive enthalpy change was recorded and when the titration of syntaxin 4 ΔTMD- L173A E174A into Munc18c was normalized to this data it was not possible to fit a model to the results. Therefore no confident conclusions can be drawn from these results. The raw data from this experiment is shown in figure 22.

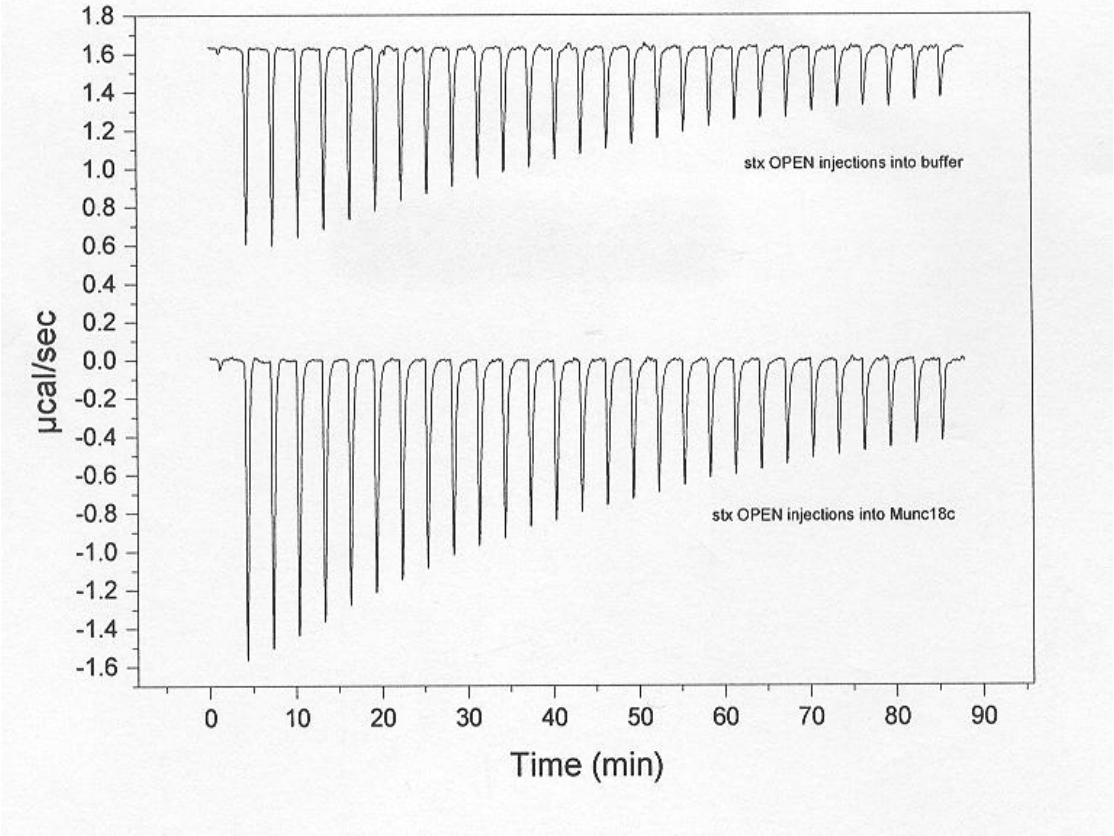


***Figure 21.*** *All ITC experiments were performed at 25 °C in PBS, pH 7.4. In A), the top panel shows the raw data in power versus time during the injections of syntaxin 4 ΔTMD-L173A E174A into a cell containing buffer alone. The lower panel shows the raw data in power versus time during the injections of syntaxin 4 ΔTMD- L173A E174A into a cell containing Munc18c. Once this data was normalized by taking into account the control experiment shown in the top graph, no model could be fitted to give K, ΔH or ΔS values*

4

Conclusions

ITC is a powerful technique that provides a large amount of information on the interactions of proteins and other small molecules. ITC has also been used, successfully to elucidate the binding of SNARE proteins showing large enthalpy changes upon the formation of the ternary neuronal SNARE complex[34]. The practicality of performing ITC experiments however is a great deal more complex that simply titrating one protein into another and recording the energy used to maintain a stable temperature. This project demonstrates the large amount of optimisation that is required to get robust believable results from ITC experiments to assess protein-protein interactions. The production of a sufficient quantity of each protein of interest at a high enough purity requires a large amount of time. The selection of the correct buffer to perform the experiments and careful dialysis to match the buffers still resulted in

large enthalpy changes in control experiments. Conclusions based upon these data therefore are not robust and the ITC experiments performed failed to provide the binding kinetics of these specific SNARE proteins. While there is no doubt that ITC techniques provide essential binding data in a variety of systems (Ghai et al 2012) it may be the case that these techniques are not applicable for assessing SNARE proteins associated with GLUT4 vesicle fusion. Although ITC has been used by others to elucidate binding of SNARE proteins (Wiederhold & Fasshauer 2009), these protein constructs were far from the endogenous full length proteins found *in vivo*. To improve solubility the authors (Wiederhold & Fasshauer 2009) removed the $H^{abc}$ domain leaving only the SNARE domain to bind. This provided valuable information on the kinetics of the interaction between only the SNARE domains but does not give any information on the binding of the rest of the proteins. Another important area that is not possible to assess using ITC is the involvement of the cell and vesicle membrane in fusion. The fusion of membranes is vital to cell survival and SNARE proteins no doubt play a key role. ITC experiments cannot incorporate the interaction of SNARE proteins and their associated membranes into the experimental design. As such comparisons of different techniques which give energy values for the fusion of membranes, and the energy generated by SNARE protein binding obtained by ITC is what is used to infer the role of SNARE proteins in vesicle fusion. Another difficulty in using ITC to obtain information of SNARE protein binding is the complexity of the SNARE complex and the order in which SNARE proteins assemble with other accessory proteins. Although SNARE proteins are thought to form the key components which drive vesicle membrane fusion, there are other proteins which bind either individual proteins or the SNARE complex during and after formation. It was the aim of this project to assess one of these proteins Munc18c to assess its role in energy landscape of SNARE protein binding. As Munc18c is thought to bind both to individual Syntaxin 4 proteins in two separate modes and to the ternary SNARE protein complex (D'Andrea-Merrins et al 2007), the use of Syntaxin 4 mutants was essential to interfere with one mode of binding and allow assessment of each individually. This was in part addressed using the constitutively open mutant of syntaxin 4: syntaxin 4 ΔTMD- L173A E174A to elucidate the binding of Munc18c to the N-terminal peptide of syntaxin 4. While this approach was necessary it proved difficult to execute in this project. The size of the proteins of interest and the difficulty with protein purity clouded any results from the experiments. This may be why other work done using ITC is done with far more truncated versions of SNARE proteins.

ITC as a method of generating binding data is almost unparalleled (Leavitt and Freire 2001) however the assay does have its limitations when used to pull apart binding in complex systems. The power of ITC lies with the ability to identify the energy required and

released upon individual molecules binding one another. When used in drug - antigen affinity screening, extremely valuable results can be obtained relatively quickly. The weaknesses of ITC therefore are not with the technique itself but with the molecules of interest used in the experiments. Great care has to be taken when using ITC to assess protein-protein interactions that the proteins are highly pure, correctly folded and in an active conformation, in an appropriate buffer to allow binding and in an appropriately high concentration. Although the work in this project went some way to address these problems, there were still enough problems to stop any robust results being obtained from the ITC experiments.

From this work on protein purification I learned that large differences in purity and quantity can be made by small changes in protocol. With regards to syntaxin 4 ΔTMD production modifying the protocols to introduce thorough wash and elution steps allowed much higher levels of purity which can be seen comparing figure 10 with figure 13. The comparison of this work to previous work done in the field (Wiederhold and Fasshauer 2009) is difficult due to the poor success of ITC experiments in this project. Also previous publications do not show figures of purified proteins and often have limited descriptions of protein purification within their methods (Wiederhold and Fasshauer 2009; D'Andrea-Merrins et al 2007). However the improvements to the protocols of recombinant protein purification are an important step forward in generating results using ITC experiments.

This work could be continued from the optimisation done in this project to assess GLUT4 vesicle associated SNARE protein interactions and provide key information alongside membrane fusion assays to the energy landscape behind SNARE complex formation and subsequent GLUT4 expression at the cell membrane. This knowledge could then be used to further the field by side by side comparisons of the different SNARE pathways in different biological systems answering questions such as: do different SNARE partners have different binding kinetics? What reasons could there be for these possible differences? Do SNARE protein mutations or SM protein mutations mediate an increased risk of type 2 diabetes? I think ITC is a very valuable tool in generating answers to these questions using the GLUT4 associated SNARE proteins and the SM protein Munc18c and if successful this project could have added valuable data on SNARE mediated GLUT4 vesicle exocytosis. Given the opportunity to continue this work further ITC experiments would have been carried out to attempt to generate more data. More work using the syntaxin 4 mutants could be done to isolate the different modes of binding to Munc18c, utilising syntaxin 4 with the N-terminal domain removed or generating mutants with the $H_{abc}$ domain removed. By sequentially performing ITC experiments with Munc18c and different syntaxin 4 constructs, lacking proposed binding sites, informative conclusions could have been made with regards to the affinities of Munc18c for the different parts of syntaxin 4.

Bibliography

1. Suzuki, K.; Kono, T., Evidence that insulin causes translocation of glucose transport activity to the plasma membrane from an intracellular storage site. *Proceedings of the National Academy of Sciences of the United States of America* **1980,** *77* (5), 2542-2547.

2. Bryant, N. J.; Govers, R.; James, D. E., Regulated transport of the glucose transporter glut4. *Nature Reviews Molecular Cell Biology* **2002,** *3* (4), 267-277.

3. Rea, S.; James, D. E., Moving GLUT4: The biogenesis and trafficking of GLUT4 storage vesicles. *Diabetes* **1997,** *46* (11), 1667-1677.

4. Smith, R. M.; Charron, M. J.; Shah, N.; Lodish, H. F.; Jarett, L., immunoelectron microscopic demonstration of insulin-stimulated translocation of glucose transporters to the plasma-membrane of isolated rat adipocytes and masking of the carboxyl-terminal epitope of intracellular GLUT4. *Proceedings of the National Academy of Sciences of the United States of America* **1991,** *88* (15), 6893-6897.

5. Ploug, T.; van Deurs, B.; Ai, H.; Cushman, S. W.; Ralston, E., Analysis of GLUT4 distribution in whole skeletal muscle fibers: Identification of distinct storage compartments that are recruited by insulin and muscle contractions. *Journal of Cell Biology* **1998,** *142* (6), 1429-1446.

6. James, D. E.; Brown, R.; Navarro, J.; Pilch, P. F., Insulin-regulatable tissues express a unique insulin-sensitive glucose-transport protein. *Nature* **1988,** *333* (6169), 183-185.

7. Zorzano, A.; Wilkinson, W.; Kotliar, N.; Thoidis, G.; Wadzinkski, B. E.; Ruoho, A. E.; Pilch, P. F., insulin-regulated glucose-uptake in rat adipocytes is mediated by 2 transporter isoforms present in at least 2 vesicle populations. *Journal of Biological Chemistry* **1989,** *264* (21), 12358-12363.

8. Pilch, P. F. In *The mass action hypothesis: formation of Glut4 storage vesicles, a tissue-specific, regulated exocytic compartment*, 10th International Symposium on Insulin Receptors and Insulin Action, Stockholm, SWEDEN, May 02-06; Blackwell Publishing: Stockholm, SWEDEN, **2007**; pp 89-101.

9. Grusovin, J.; Macaulay, S. L., Snares for GLUT4 - Mechanisms directing vesicular trafficking of GLUT4. *Frontiers in Bioscience* **2003,** *8*, D620-D641.

10. Shi, J.; Kandror, K. V. In Sortilin is essential and sufficient for the formation of insulin-responsive Glut4-storage vesicles, 65th Annual Meeting of the American-Diabetes-Association, San Diego, CA, Jun 10-14; Amer Diabetes Assoc: San Diego, CA, **2005**; pp A71-A71.

11. Watson, R. T.; Kanzaki, M.; Pessin, J. E., Regulated membrane trafficking of the insulin-responsive glucose transporter 4 in adipocytes. *Endocrine Reviews* **2004,** *25* (2), 177-204.

12. Jahn, R.; Scheller, R. H., SNAREs - engines for membrane fusion. *Nature Reviews Molecular Cell Biology* **2006,** *7* (9), 631-643.

13. Weimbs, T.; Low, S. H.; Chapin, S. J.; Mostov, K. E.; Bucher, P.; Hofmann, K., A conserved domain is present in different families of vesicular fusion proteins: A new superfamily. *Proceedings of the National Academy of Sciences of the United States of America* **1997,** *94* (7), 3046-3051.

14. Sutton, R. B.; Fasshauer, D.; Jahn, R.; Brunger, A. T., Crystal structure of a SNARE complex involved in synaptic exocytosis at 2.4 angstrom resolution. *Nature* **1998,** *395* (6700), 347-353.

15. Katz, L.; Brennwald, P., Testing the 3Q : 1R "rule": Mutational analysis of the ionic "zero" layer in the yeast exocytic SNARE complex reveals no requirement for arginine. *Molecular Biology of the Cell* **2000,** *11* (11), 3849-3858.

16. Dietrich, L. E. P.; Boeddinghaus, C.; LaGrassa, T. J.; Ungermann, C., Control of eukaryotic membrane fusion by N-terminal domains of SNARE proteins. *Biochimica Et Biophysica Acta-Molecular Cell Research* **2003,** *1641* (2-3), 111-119.

17. Yamaguchi, T.; Dulubova, I.; Min, S. W.; Chen, X. H.; Rizo, J.; Sudhof, T. C., Sly1 binds to Golgi and ER syntaxins via a conserved N-terminal peptide motif. *Developmental Cell* **2002,** *2* (3), 295-305.

18. Hong, W. J., SNAREs and traffic (vol 1744, pg 120, 2005). *Biochimica Et Biophysica Acta-Molecular Cell Research* **2005,** *1744* (3), 465-+.

19. Sollner, T.; Bennett, M. K.; Whiteheart, S. W.; Scheller, R. H.; Rothman, J. E., A protein assembly-disassembly pathway in-vitro that may correspond to sequential steps of synaptic vesicle docking, activation, and fusion. *Cell* **1993,** *75* (3), 409-418.

20. Mayer, A.; Wickner, W.; Haas, A., Sec18p (NSF)-driven release of Sec17p (alpha-SNAP) can precede docking and fusion of yeast vacuoles. *Cell* **1996,** *85* (1), 83-94.

21. Fasshauer, D.; Margittai, M., A transient N-terminal interaction of SNAP-25 and syntaxin nucleates SNARE assembly. *Journal of Biological Chemistry* **2004,** *279* (9), 7613-7621.

22. Hata, Y.; Slaughter, C. A.; Sudhof, T. C., Synaptic vesicle fusion complex contains unc-18 homologue bound to syntaxin. *Nature* **1993,** *366* (6453), 347-351.

23. Misura, K. M. S.; Scheller, R. H.; Weis, W. I., Three-dimensional structure of the neuronal-Sec1-syntaxin 1a complex. *Nature* **2000,** *404* (6776), 355-362.

24. Brenner, S., genetics of caenorhabditis-elegans. *Genetics* **1974,** *77* (1), 71-94.

25. Nicholson, K. L.; Munson, M.; Miller, R. B.; Filip, T. J.; Fairman, R.; Hughson, F. M., Regulation of SNARE complex assembly by an N-terminal domain of the t-SNARE Sso1p. *Nature Structural Biology* **1998,** *5* (9), 793-802.

26. Dulubova, I.; Yamaguchi, T.; Wang, Y.; Sudhof, T. C.; Rizo, J., Vam3p structure reveals conserved and divergent properties of syntaxins. *Nature Structural Biology* **2001,** *8* (3), 258-264.

27. Deak, F.; Xu, Y.; Chang, W.-P.; Dulubova, I.; Khvotchev, M.; Liu, X.; Sudhof, T. C.; Rizo, J., Munc18-1 binding to the neuronal SNARE complex controls synaptic vesicle priming. *J. Cell Biol.* **2009,** *184* (5), 751-764.

28. Rea, S.; Martin, L. B.; McIntosh, S.; Macaulay, S. L.; Ramsdale, T.; Baldini, G.; James, D. E., Syndet, an adipocyte target SNARE involved in the insulin-induced translocation of GLUT4 to the cell surface. *Journal of Biological Chemistry* **1998,** *273* (30), 18784-18792.

29. Zhao, P.; Yang, L.; Lopez, J. A.; Fan, J.; Burchfield, J. G.; Bai, L.; Hong, W.; Xu, T.; James, D. E., Variations in the requirement for v-SNAREs in GLUT4 trafficking in adipocytes. *Journal of Cell Science* **2009,** *122* (19).

30. Tellam, J. T. ;Macaulay, S. L. ;McIntosh, S. ;Hewish, D. R. ;Ward, C. W. ;James, D. E., Characterization of Munc-18c and syntaxin-4 in 3T3-L1 adipocytes - Putative role in insulin-dependent movement of GLUT-4. *Journal of Biological Chemistry,* **1997,** *272,* (10)

31. Brandie, F. M.; Aran, V.; Verma, A.; McNew, J. A.; Bryant, N. J.; Gould, G. W., Negative regulation of syntaxin4/SNAP-23/VAMP2-mediated membrane fusion by Munc18c in vitro. *PLoS ONE* **2008,** *3* (12), e4074.

32. Bracher, A.; Weissenhorn, W., Structural basis for the Golgi membrane recruitment of Sly1p by Sed5p. *Embo Journal* **2002,** *21* (22), 6114-6124.

33. Catherine F. Latham, J. A. L., Shu-Hong Hu, Christine L. Gee, Elizabeth Westbury, Duncan H. Blair, Chris J. Armishaw, Paul F. Alewood, Nia J. Bryant, David E. James, Jennifer L. Martin,, Molecular Dissection of the Munc18c/Syntaxin4 Interaction: Implications for Regulation of Membrane Trafficking. *Traffic* **2006,** *7* (10), 1408-1419.

34. Hu, S. H.; Latham, C. F.; Gee, C. L.; James, D. E.; Martin, J. L., Structure of the Munc18c/Syntaxin4 N-peptide complex defines universal features of the N-peptide binding mode of Sec1/Munc18 proteins. *Proceedings of the National Academy of Sciences of the United States of America* **2007,** *104* (21), 8773-8778.

35. D'Andrea-Merrins M., Chang L., Lam A. D., Ernst S. A., Stuenkel E. L., Munc18c Interaction with Syntaxin 4 Monomers and SNARE Complex Intermediates in GLUT4 Vesicle Trafficking. *The Journal of Biological Chemistry,* **2007,** *282,* 16553-16566

36 Dulubova I., Sugita S., Hill S., Hosaka M., Fernandez I., Sudorf T. C., Rizo J., A conformational switch in syntaxin during exocytosis. *The EMBO Journal,* **1999**, *18*, (16) 4372-4382

37. Aran, V ;Brandie, FM ;Boyd, AR ;Kantidakis, T ;Rideout, EJ ;Kelly, SM ;Gould, GW ;Bryant, N., Characterisation of two distinct binding modes between Syntaxin 4 and Munc18c., *Biochemical Journal,* **2009,** *419* (3) 655-660

38 Richmond J. E., Weimer R. M., Jorgensen E. M., An open form of syntaxin bypasses the requirement for UNC-13 in vesicle priming. *Nature,* **2001,** *412,* (6844) 338-341

39. Wiederhold, K.; Fasshauer, D., Is Assembly of the SNARE Complex Enough to Fuel Membrane Fusion? *Journal of Biological Chemistry* **2009,** *284* (19), 13143-13152.

40. Jewell, J. L.; Oh, E.; Bennett, S. M.; Meroueh, S. O.; Thurmond, D. C., The tyrosine phosphorylation of Munc18c induces a switch in binding specificity from syntaxin 4 to Doc2 beta. *Journal of Biological Chemistry* **2008,** *283* (31).

41. Ghai R., Falconer R. J., Collins B. M., Applications of isothermal titration calorimetry in pure and applied research--survey of the literature from 2010. *Journal of Molecular Recognition*, **2012,** *25* (1) 32-52

42 Leavitt S., Freire E., Direct measurement of protein binding energetics by isothermal titration calorimetry. *Current Opinion in Structural Biology***, 2001,** 11 560-566

43 Craig T. J., Ciufo L. F., Morgan A. A protein–protein binding assay using coated microtitre plates: increased throughput, reproducibility and speed compared to bead-based assays. *Journal of Biochemical and Biophysical Methods,* **2004**, 60 (1) 49-60

44 Fasshauer D., Antonin W., Margittai M., Pabst S. and Jahn R. Mixed and Non-cognate SNARE Complexes CHARACTERIZATION OF ASSEMBLY AND BIOPHYSICAL PROPERTIES. *The Journal of Biological Chemistry*, **1999,** 274 15440-15446

45 Barclay J. W., . Craig T. J., Fisher R. J., Ciufo L. F., Evans G. J. O., Morgan A., and Burgoyne R. D. Phosphorylation of Munc18 by Protein Kinase C Regulates the Kinetics of Exocytosis. *The Journal of Biological Chemistry*, **2003,** 278, 10538-10545

46 Terpe K. Overview of tag protein fusions: from molecular and biochemical fundamentals to commercial systems. *Applied Microbiology and Biotechnology,* **2003,** 60 523-533

47 Ravichandran V., Chawla A., Roche P. A. Identification of a Novel Syntaxin- and Synaptobrevin/VAMP-binding Protein, SNAP-23, Expressed in Non-neuronal Tissues. *The Journal of Biological Chemistry,* **1996,** 271 13300-13303

48 Foster L. J., Yeung B., Mohtashami M., Ross K., Trimble S. W. and Klip A. Binary Interactions of the SNARE Proteins Syntaxin-4, SNAP23, and VAMP-2 and Their Regulation by Phosphorylation. *Biochemistry,* **1998,** 37 (31) 11089-11096